

THESIS

SEASONAL GREENING IN GRASSLANDS

Submitted by

Biljana Orescanin

Department of Atmospheric Science

In partial fulfillment of the requirements

For the Degree of Master of Science

Colorado State University

Fort Collins, Colorado

Summer 2013

Master's Committee:

Advisor: A. Scott Denning

David A. Randall
Keith H. Paustian

Copyright by Biljana Orescanin 2013

All Rights Reserved

ABSTRACT

SEASONAL GREENING IN GRASSLANDS

Grasslands cover about one quarter of the Earth's land and are currently considered to act as carbon sinks, taking up an estimated 0.5 Gt C per year. Thus, robust understanding of the grassland biome (e.g. representation of seasonal cycle of plant growth and the amount of green mass, often referred to as phenology, in global carbon models) plays a key role in understanding and predicting the global carbon cycle.

The focus of this research is on improvement of a grassland biome representation in a biosphere model, which sometimes fails to correctly represent the phenology of vegetation. For this purpose, as a part of Simple Biosphere model (SiB3), a phenology model is tested and improved to provide more realistic representation of plant growth dependence on available moisture, which along with temperature and light controls plant growth. The new methodology employs integrated soil moisture in plant growth simulation. This new representation addresses the nature of the plants to use their root system to access the water supply. At same time it represents the plant's moisture recourses more accurately than the currently used vapor pressure method, which in grasslands is often non-correlated with soil conditions. The new technique has been developed and tested on data from the Skukuza flux tower site in South Africa and evaluated at 6 different flux tower sites around the world covering a variety of climate conditions. The technique is relatively easy and inexpensive to implement into the existing model providing excellent results capturing both the onset of green season and greening

cycle at all locations. Although the method is developed for grasslands biome its representation of natural plant processes provides a good potential for its global use.

ACKNOWLEDGEMENTS

I would like to acknowledge and greatly thank the following people who have made the completion of my thesis possible:

I thank my advisor, Dr. A. Scott Denning, for valuable support, helpful discussions, and comments during the entire process of writing this thesis and also for the opportunity to work with the best scientists in our field. I also thank my committee members, Dr. David A. Randall and Dr. Keith H. Pustian, for their interest in my research.

I very much appreciate and gratefully acknowledge Dr. Ian T. Baker for his invaluable assistance and suggestions, which were indispensable for the successful accomplishment of my thesis. I am very grateful to the Biocycle Group for all of their support and encouragement, especially Erica McGrath-Spangler, Isaac Medina and Parker Kraus.

I am grateful for the support and understanding from my family and friends.

This work has been supported by the National Science Foundation/Collaboration in Mathematical Geosciences (#ATM-0930265), Science and Technology Center for MultiScale Modeling of Atmospheric Processes, managed by Colorado State University under cooperative agreement (#ATM-0425247).

TABLE OF CONTENTS

	<u>Page</u>
CHAPTER 1 INTRODUCTION.....	1
CHAPTER 2 DATA AND MODEL DESCRIPTION	10
2.1 MODEL DESCRIPTION	10
2.1.1 <i>The Simple Biosphere Model (SiB)</i>	10
2.1.2 <i>Phenology model</i>	16
2.2 DATA.....	20
2.2.1 <i>Site descriptions</i>	21
2.2.2 <i>Tower data</i>	26
CHAPTER 3 METHODOLOGY.....	29
3.1 DETECTION OF THE START AND END OF GREENING SEASON	29
3.2 NEW METHODOLOGY FOR CALCULATING GROWING SEASON INDEX (GSI)	31
3.3 EVALUATION	37
CHAPTER 4 RESULTS AND DISCUSSION.....	38
4.1 DETECTION OF GREENING SEASON	38
4.2 PREDICTION OF GREENING SEASON	41
4.2.1 <i>GSI and its contributing factors</i>	41
4.2.2 <i>Leaf Area Index – LAI</i>	44
4.3 EVALUATION	45
CHAPTER 5 CONCLUSIONS	64
REFERENCES	66
APPENDIX A	80
APPENDIX B	87

LIST OF TABLES

<u>Table</u>	<u>Page</u>
Measurements site abbreviations, locations, and principal investigators.....	21
Skukuza tower data used in the study; original units (as provided from the site); what the data are used for	28
Distribution of phenological functional types present at S0 - Skukuza site.....	41
A List of 35 phenology types allowed in SiB's phenology model.....	87
Distribution of phenological functional types present at site S0 – Skukuza, Kruger Park, South Africa.....	88
Distribution of phenological functional types present at S1 – Lethbridge, Canada	88
Distribution of phenological functional types present at site S2 - Shidler Tallgrass Prairie, Oklahoma, US.....	88

LIST OF FIGURES

<u>Figure</u>	<u>Page</u>
Observations of atmospheric CO ₂ concentration (ppm) at Mauna Loa observatory over last half a century. Source: Scripps Institution of Oceanography NOAA Earth System Research Laboratory.....	2
Schematic Simple Biosphere Model, version 3 (SiB3).....	13
Spatial distribution of different vegetation in SiB model: 1- <i>Broadleaf evergreen</i> ; 2- <i>Deciduous Broadleaf Trees</i> ; 3- <i>Mixed forest</i> ; 4- <i>Needleleaf/pine tree</i> ; 5- <i>Needleleaf deciduous</i> ; 6- <i>Broadleaf with ground cover</i> ; 7- <i>Ground cover/maize optical</i> ; 8 - <i>Not used</i> ; 9 - <i>Shrubs</i> ; 10 - <i>Tundra</i> ; 11 - <i>Low-latitude desert</i> ; 12- <i>Crop</i>	15
Measurements site locations.....	20
Change in GSI 10-day running mean contributors at Skukuza site in year 2002.....	30
Comparison between different 10-day running mean forecasted and observed parameters and their relation to detected start (SOS) and end (EOS) of greening season; green triangles – SOS; yellow triangles – EOS; each of detected greening seasons is shaded; tbarflx- temperature; br- Bowen ratio; sm16bacac – soil moisture at 16cm depth; rain – rainfall accumulation; zlt MODIS – leaf area index detected by MODIS; Fpar MODIS – Fpar detected by MODIS; pawfrac SiB - plant available water fraction diagnosed by SiB	40
Growing Season Index –GSI (in black) and its contributors: temperature, light and moisture factors (in red, blue and green, respectively) at Skukuza site for time period from January 1 st 2000 to December 31 st 2005, given by SiB3 using <i>vpd-method</i> (upper plot) and <i>pawfrac-method</i> (lower plot). All values are 10-day running means.	42
Rain (top, red) and LAI (at bottom with y-axes on the right) at Skukuza site for time period from January 1 st 2000 to December 31 st 2005. Vpd-method LAI is given by green dotted line while pawfrac-method is given by blue dashed line. All values are 10-day running means. Shaded areas denote greening seasons as detected by criteria defined in Chapter 3.....	44
Comparison of the observed (red) and forecasted fluxes (from the top: Latent Heat, Sensible Heat and Carbon) produced by <i>vpd-method</i> (green) and <i>pawfrac-method</i> (blue), precipitation (second from the bottom), and LAI (the bottom plot) [observed (crosses) and forecasted (<i>vpd-mehtod</i> in green, <i>pawfrac-method</i> in blue)] for site S0 - Skukuza, Kruger Park, South Africa for period January 1 st 2000 till December 31 st 2005.	47
Growing Season Index –GSI (in black) and its contributors: temperature, light and moisture factors (in red, blue and green, respectively) at Lethbridge, Canada for time period from January 1 st 1997 to December 31 st 2006, given by SiB3 using <i>vpd-method</i> (upper plot) and <i>pawfrac-method</i> (lower plot). All values are 10-day running means.	49
Comparison of the observed (red) and forecasted fluxes (from the top: Latent Heat, Sensible Heat and Carbon) produced by <i>vpd-method</i> (green) and <i>pawfrac-method</i> (blue), precipitation (second from the bottom), and LAI (the bottom plot) [observed	

(crosses) and forecasted (<i>vpd-mehtod</i> in green, <i>pawfrac-method</i> in blue)] for site S1 - Lethbridge, Canada for period January 1 st 1997 till December 31 st 2006.....	50
Growing Season Index -GSI (in black) and its contributors: temperature, light and moisture factors (in red, blue and green, respectively) at Shidler Tallgrass Prairie, Oklahoma, US for time period from January 1 st 1997 to December 31 st 2000, given by SiB3 using <i>vpd-method</i> (upper plot) and <i>pawfrac-method</i> (lower plot). All values are 10-day running means.....	52
Comparison of the observed (red) and forecasted fluxes (from the top: Latent Heat, Sensible Heat and Carbon) produced by <i>vpd-method</i> (green) and <i>pawfrac-method</i> (blue), precipitation (second from the bottom), and LAI [(the bottom plot) - observed (crosses) and forecasted (<i>vpd-mehtod</i> in green, <i>pawfrac-method</i> in blue)] for site S2 - Shidler Tallgrass Prairie, Oklahoma, US for period between January 1 st 1997 till December 31 st 2000	54
Growing Season Index -GSI (in black) and its contributors: temperature, light and moisture factors (in red, blue and green, respectively) at Fermi Prairie, Illinois, US for time period from January 1 st 2004 to December 31 st 2007, given by SiB3 using <i>vpd-method</i> (upper plot) and <i>pawfrac-method</i> (lower plot). All values are 10-day running means.....	55
Comparison of the observed (red) and forecasted fluxes (from the top: Latent Heat, Sensible Heat and Carbon) produced by <i>vpd-method</i> (green) and <i>pawfrac-method</i> (blue), precipitation (second from the bottom), and LAI [(the bottom plot) - observed (crosses) and forecasted (<i>vpd-mehtod</i> in green, <i>pawfrac-method</i> in blue)] for site S3 - Fermi Prairie, Illinois, US for period between January 1 st 2004 till December 31 st 2007	56
Growing Season Index -GSI (in black) and its contributors: temperature, light and moisture factors (in red, blue and green, respectively) at <i>Vaira Ranch, California, US</i> for time period from January 1 st 2001 to December 31 st 2007, given by SiB3 using <i>vpd-method</i> (upper plot) and <i>pawfrac-method</i> (lower plot). All values are 10-day running means.....	57
Comparison of the observed (red) and forecasted fluxes (from the top: Latent Heat, Sensible Heat and Carbon) produced by <i>vpd-method</i> (green) and <i>pawfrac-method</i> (blue), precipitation (second from the bottom), and LAI [(the bottom plot) - observed (crosses) and forecasted (<i>vpd-mehtod</i> in green, <i>pawfrac-method</i> in blue)] for site S4 - Vaira Ranch, California, US for period between January 1 st 2001 till December 31 st 2007	58
Growing Season Index -GSI (in black) and its contributors: temperature, light and moisture factors (in dotted black, blue and green, respectively) at <i>Fort Pack, Montana, US</i> for time period from January 1 st 2000 to December 31 st 2007, given by SiB3 using <i>vpd-method</i> (upper plot) and <i>pawfrac-method</i> (lower plot). All values are 10-day running means.....	59
Comparison of the forecasted fluxes (from the top: Latent Heat, Sensible Heat and Carbon) produced by <i>vpd-method</i> (green) and <i>pawfrac-method</i> (blue), precipitation from driver's data (second from the bottom), and forecasted LAI (the bottom plot, <i>vpd-mehtod</i> in green, <i>pawfrac-method</i> in blue) for site S5 - Fort Peck, Montana, US for period January 1 st 2000 till December 31 st 2007	60

Growing Season Index –GSI (in black) and its contributors: temperature, light and moisture factors (in dotted black, blue and green, respectively) at Fazenda Nossa Senhora, Brazil for time period from January 1 st 1999 to December 31 st 2001, given by SiB3 using <i>vpd-method</i> (upper plot) and <i>pawfrac-method</i> (lower plot). All values are 10-day running means.....	61
Comparison of the observed (red) and forecasted fluxes (from the top: Latent Heat, Sensible Heat and Carbon) produced by <i>vpd-method</i> (green) and <i>pawfrac-method</i> (blue), precipitation from driver's data (second from the bottom), and LAI [(the bottom plot) forecasted <i>vpd-method</i> in green, <i>pawfrac-method</i> in blue] for site S6 - Fazenda Nossa Senhora, Brazil for period January 1 st 1999 till December 31 st 2001.....	62
Observed LAI (dotted line with filled rhomboids) at S6 - Fazenda Nossa Senhora, Brazil for period January 1 st 1999 till December 31 st 2005. After Zanchi et al. (2009). IAF on y-axes stands for LAI. X-axes is time in 6 month increments labeled by year.....	63
Monthly means of observed (red) and modeled (blue) variables at site S0 – Skukuza, Kruger Park, South Africa. LW – Long Wave radiation; SW – Short Wave radiation; SH Sensible Heat; LH – Latent Heat; Nee cflux SiB – carbon flux diagnosed by SiB; LAI – Leaf Area Index.....	80
Monthly means of observed (red) and modeled (blue) variables at site S1 – Lethbridge, Canada. LW – Long Wave radiation; SW – Short Wave radiation; SH Sensible Heat; LH – Latent Heat; Nee cflux SiB – carbon flux diagnosed by SiB; LAI – Leaf Area Index.....	81
Monthly means of observed (red) and modeled (blue) variables at site S2 – Shidler Tallgrass Prairie, Oklahoma, US. LW – Long Wave radiation; SW – Short Wave radiation; SH Sensible Heat; LH – Latent Heat; Nee cflux SiB – carbon flux diagnosed by SiB; LAI – Leaf Area Index.....	82
Monthly means of observed (red) and modeled (blue) variables at site S3 – Fermi Prairie, Illinois, US. LW – Long Wave radiation; SW – Short Wave radiation; SH Sensible Heat; LH – Latent Heat; Nee cflux SiB – carbon flux diagnosed by SiB; LAI – Leaf Area Index.....	83
Monthly means of observed (red) and modeled (blue) variables at site S4 – Vaira Ranch, California, US. LW – Long Wave radiation; SW – Short Wave radiation; SH Sensible Heat; LH – Latent Heat; Nee cflux SiB – carbon flux diagnosed by SiB; LAI – Leaf Area Index.....	84
Monthly means of observed (red) and modeled (blue) variables at site S5 – Fort Peck, Montana, US. LW – Long Wave radiation; SW – Short Wave radiation; SH Sensible Heat; LH – Latent Heat; Nee cflux SiB – carbon flux diagnosed by SiB; LAI – Leaf Area Index.....	85
Monthly means of observed (red) and modeled (blue) variables at site S6 – Fazenda Nossa Senhora, Brazil. LW – Long Wave radiation; SW – Short Wave radiation; SH Sensible Heat; LH – Latent Heat; Nee cflux SiB – carbon flux diagnosed by SiB; LAI – Leaf Area Index.....	86

CHAPTER 1 Introduction

According to the Fourth Assessment Report by the Intergovernmental Panel on Climate Change (IPCC) from 2007 the increase in the concentration of carbon dioxide (CO_2) in the atmosphere (Keeling, 1995, IPCC 2007) is caused by human activity, mainly in the form of fossil fuel burning, cement production, and land cover/land- use change. Although the exact nature of global response is uncertain, radiative forcing imposed by this increase in greenhouse gases is predicted to change the Earth's climate (Solomon *et al.*, 2009, IPCC 2007;). Figure 1 shows the atmospheric concentration of CO_2 at Mauna Loa observatory, Hawaii, over the last half a century. The increase in CO_2 concentration is a consequence of fossil fuel burning, which has increased both marine and terrestrial consumption of CO_2 . Global consumption, naturally, has to be balanced by global carbon sinks, however, these are not well known at the moment. The so-called missing sink of CO_2 which accounts for about half of the anthropogenic CO_2 emission in a given year (Keeling, 1995; IPCC 2007) is still unexplained. While maritime CO_2 flux is relatively constant (Friedlingstein *et al.*, 2006), terrestrial CO_2 flux is highly variable in both space and time. Therefore, current efforts to locate and understand the missing CO_2 sink are primarily focused to land. The uncertainty in the land behavior under future climate is such that it is not currently resolved whether the land will be a net source or sink of carbon. A significant contribution to this uncertainty is coming from the fact that the terrestrial biosphere is not completely understand yet and many possible aspects of land to atmosphere interactions are left to be explained.

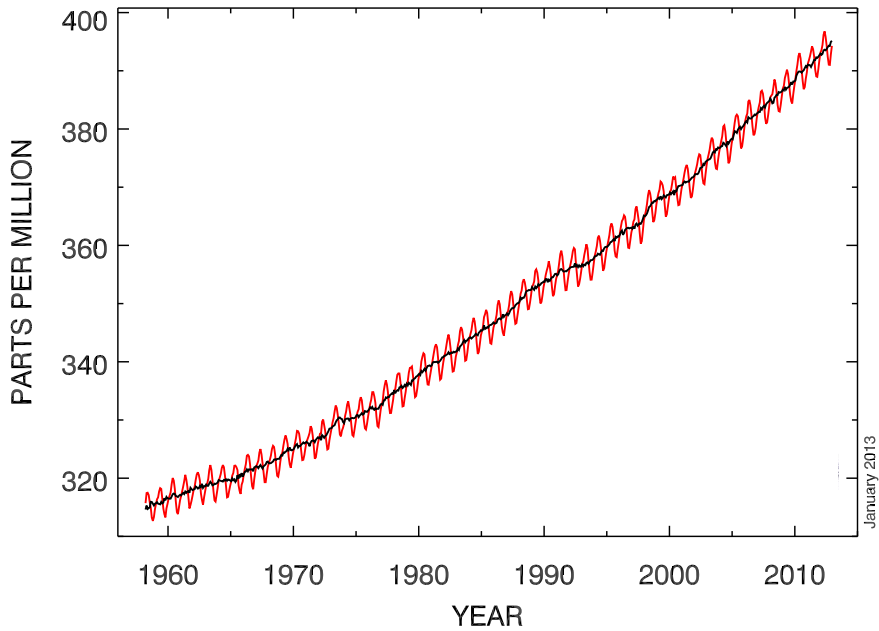


Figure 1 Observations of atmospheric CO₂ concentration (ppm) at Mauna Loa observatory over last half a century. Source: Scripps Institution of Oceanography NOAA Earth System Research Laboratory.

With no doubt the terrestrial biosphere plays an important role in the global carbon cycle. Since the 1994 IPCC, there has been an effort to improve the quantification of terrestrial exchanges and potential feedbacks from climate, changing CO₂, and other factors. Lack of knowledge about positive and negative feedbacks from the biosphere is among major limiting factors to credible simulations of future atmospheric CO₂ concentrations. Analyses of the atmospheric gradients and concentrations of CO₂ provide increasingly strong evidence for terrestrial sinks, potentially distributed between Northern Hemisphere and tropical regions, but conclusive detection in direct biomass and soil measurements remains elusive.

Current regional-to-global terrestrial ecosystem models with coupled carbon and nitrogen cycles represent the effects of CO₂ fertilization differently, but all suggest long-term responses to CO₂ that are substantially smaller than potential leaf-level or laboratory

whole plant-level responses (Schimel, 2006). Analyses of emissions and biogeochemical fluxes consistent with eventual stabilization of atmospheric CO₂ concentrations are sensitive to the way in which biospheric feedbacks are modeled. Decisions about land use can have effects of 100s of Giga tons of carbon (Gt C) over the next few centuries, with similarly significant effects on the atmosphere. Therefore, a major role that terrestrial ecosystems play in the global carbon cycle is critical for the understanding of terrestrial carbon metabolism.

Ecosystems are usually grouped into biomes or plant functional types, which reflect natural geographic differences in soils and climate, and consequently different vegetation types (Woodward et al. 2004, Stöckli et al. 2011). These biomes differ greatly in their capacity to assimilate and store carbon (De Deyn et al. 2008), and it is preferred to treat them separately in ecosystem simulations. In each of the biomes, in addition to the balance of carbon gains through growth and losses through respiration, ecosystem carbon balance is regulated by several other factors including fire, herbivores, erosion, and leaching.

The amount of carbon stored above ground depends on how much bio mass there is, and can range from less than 2×10^{-9} Gt C per hectare for tropical grasslands to over 30×10^{-9} Gt C per hectare for woodland savannas. Root carbon stocks tend to be slightly higher, with estimates of $7 - 54 \times 10^{-9}$ Gt C per hectare, while soil carbon stocks are even higher $\sim 174 \times 10^{-9}$ Gt C per hectare (Grace et al. 2006). When dealing with savannas and tropical grasslands it is worth mentioning that even they are naturally subject to frequent fires, which are an important component in the functioning of these ecosystems (fire events in savannas can release huge amounts of carbon to the atmosphere estimated at 0.5–4.2 Gt C per year globally) the carbon lost due to the fire events is mostly regained during the

subsequent period of plant regrowth (Grace et al. 2006) and these ecosystems are currently considered to act overall as carbon sinks, taking up an estimated 0.5 Gt C per year (Scurlock and Hall 1998). Thus, better understanding of the grassland biome (e.g. better representation of phenological properties in global carbon models) plays a key role in understanding and predicting the global carbon cycle (Richardson et al, 2012). Therefore, the focus of this research is on a single biome – grassland, and an improvement of its representation in the biosphere models. As will be presented latter, biosphere models often fail to correctly represent seasonality and amount of green mass, especially in rain driven biomes such as grassland.

Grasslands, also known as prairies in the U.S. Midwest, pampas in South America, steppes in the Central Eurasian and savannas in Africa, cover about one quarter of the Earth's land. Their soils tend to be deep and fertile, perfect for cropland or pastures. In general, they are open and fairly flat, being present on every continent except Antarctica. Most lie in the drier portions of a continent's interior and can be found where there is not enough regular rainfall to support the growth of a forest, but not so little as to form a desert. In fact, most grasslands are located between forests and deserts, with those in the southern hemisphere tending to get more precipitation than those in the northern hemisphere (Gibson, 2009).

Savannas are spatially and temporally complex systems in which woody vegetation (i.e. trees) and herbaceous vegetation (i.e. grasses) both contribute significantly to system level functions (e.g. primary production, carbon, water, and nutrient cycling). Savanna regions are also subject to changes in the balance between woody and herbaceous covers that remain poorly understood and can have large impacts on land surface- atmosphere interactions and system biogeochemistry. They occur in regions with strongly alternating

wet and dry seasons (Mistry 2000), with rainfall ranging from 300 to 2000 mm yr⁻¹. At local scales, savannas are modulated by soil water content and drainage, nutrient availability, disturbance regimes, and land use change (Scholes and Archer 1997). These factors combine to produce a large diversity of species and functional groups, vegetation structure (e.g., height, cover, leaf area index (LAI), albedo, and surface roughness), phenology, and plant physiology (e.g., leaf properties, water, and light use efficiency). These characteristics affect biophysical processes, and hence the fluxes of mass and energy to the atmosphere. In the savanna region, gross vegetation changes (reduced LAI) resulting from burning have been shown to alter local and regional climate (Lynch et al. 2007; Görge et al. 2006). However, most climate models used in the IPCC Fourth Assessment Report (Randall et al. 2007) treat all savannas as a single vegetation/biome type, and therefore do not adequately capture the variability of savanna structure, composition, and function. Many of these models fail to capture the seasonality of fluxes in savannas because they cannot simulate the complex interactions between rainfall, soil moisture, root distribution, and plant water uptake (Pitman 2003). There is, therefore, a vital need to understand what the climatic and biophysical thresholds that maintain the biosphere are, and how the resilience of the biosphere to future atmospheric change can be enhanced.

Most of the savanna areas are natural ecosystems characterized as the co-dominance of trees and grasses, ranging from grasslands, where trees are virtually absent, to more forest-like ecosystems, where trees are dominant, the savanna biome represents a daunting diversity of vegetation associations and arrangements. However, savannas can also be formed by the degradation of tropical forests from burning, grazing, and deforestation. Mixture of vegetation with that large variety of phenological types has been,

and still is, a real challenge when it comes to complete understanding of its nature. Also, due to adaptation and evolution process, one vegetation type does not respond to environmental changes equally at all climates. Ecosystems are not just static elements of the landscape; they are dynamic. The biomass of plant species changes over periods of years to centuries. Disturbances such as floods and fires are natural features of landscapes and initiate temporal changes in ecosystems known as succession. The life history patterns of plants have evolved in part as a result of recurring disturbances. Many plant species are ephemeral members of the landscape, adapted to recently disturbed sites. Others dominate old-growth ecosystems in the late stages of succession. Long-term changes in temperature, precipitation, atmospheric CO₂, and the chemistry of precipitation alter the conditions for processes such as photosynthesis and respiration, reproduction, and nutrient availability (Bonan, 2002). Therefore, plant's phenology has to be addressed with spatial dependence.

One of the key aspects for successful simulation of a biome such as savanna is the onset and the length of the green season. The timing and duration of leaf display affect a range of ecosystem processes – from carbon, water, and energy exchange to forage availability. A delay of a few weeks in the production of new leaves can cause a difference to the survival and reproductive success of the herbivores that depend on them (Owen-Smith and Cooper 1989). The onset of greening season (hereafter a Start Of the Season, or SOS) of any biome depends mostly on three conditions: light, temperature and moisture. A correct combination of these three triggers the greening. However, different regions do not experience same oscillations in all of the parameters listed above.

Environmental cues of leaf phenology are well understood in temperate systems (Cannell and Smith 1983; Chuine and Cour 1999; Nizinski and Saugier 1988; Seiwa 1999).

Temperature and photoperiod (day length) control phenology in the high latitudes, but there are conflicting opinions on their importance in systems like tropical savannas where water, not temperature or light, is often the limiting factor for growth (Scholes and Walker 1993). Tropical savanna is a key terrestrial biome that dominates 15% of the global land surface and warrants special attention because of its vast spatial extent, high productivity, rapid carbon turnover, vulnerability to climate change (which can alter fire regimes and water availability), poor management (i.e., high population pressures and overutilization for grazing and firewood), and land use change (Canadell et al. 2003).

Predicting savanna phenological patterns is complicated for two reasons. Firstly, although water availability is identified as an important seasonal driver (Reich and Borchert 1984; Singh and Kushwaha 2005), it is difficult to measure at regional scales. Rainfall data and calculations of potential evapotranspiration both fall short – rainfall because it reflects only the input side of the water balance and is an episodic rather than continuous variable, and potential evapotranspiration because it is not known how much water is present to be evaporated.

Unlike in temperate systems – where low winter temperatures pose a barrier to growth of most plant-types – in rainfall-driven systems, such as savannas, there is the potential for a range of different strategies, depending on an organism's ability to store/access water. Thus, seasonal responses of savanna plant species are closely linked to their structure and function. Many tree species are known to put on leaves before the first rains of the season (Do et al. 2005; Shackleton 1999; Milton 1987), whereas growth of grasses is always limited by water availability (Dye and Walker 1987; Prins 1988). Because trees and grasses have different seasonal patterns of leaf display, the largescale, long term datasets provided

by satellite imagery (Reed et al. 1994) are of little use in savannas, unless it is possible to separate the contributions of these two main functional types to the landscape greenness.

Describing soil moisture availability and separating tree and grass responses have been identified as the two main factors limiting our ability to model canopy dynamics in savanna systems (Jolly and Running 2004). This research is an attempt of resolving this issue by finding a more physical relationship between available water and an onset of green season in grasslands through land-surface and phenology model simulations, having the main focus on grass, with trees not being ignored. These models, currently, use a growth seasonal index, GSI, to represent the rate at which certain plant-functional types grow (Stöckli et al. 2011). This quantity is, however, calculated based on the atmospheric moisture condition. In savannas this results in poorly captured seasonal change of LAI between dry and wet periods, proving that atmospheric moisture is not a good indicator of green season onset in precipitation-governed biomes.

The reason is most likely in the fact that atmospheric moisture is not only a function of rainfall but to a number of other factors such as atmospheric moisture advection, soil moisture and soil capability to keep the moisture closer to the surface where it influences a relative humidity of the air. In order to improve our ability to model canopy dynamics in savanna systems this study employs information on soil moisture more directly as suggested by Archibald and Scholes (2007). A *plant available water fraction (pawfrac)*, which represents the fraction of the water that is available to the plant compared to the maximum possible amount of water that given soil can hold is used to better estimate both start and end of the green season of savannas. This should significantly improve a greening cycle simulations and setup better base for feedbacks of carbon consumptions being

beneficial for our understanding of land to atmosphere interaction in grasslands. A current atmospheric moisture condition that is used to estimate GSI is attractive because it is available from reanalysis data but it is not physically or biologically connected to plant growth. Soil moisture on the other side represents a time integral response to seasonal rainfall. It's lagged and smoothed compared to precipitation and best of all it's biologically related to plant growth.

The research is an observational-modeling study that focuses on understanding the greening seasonality of grasslands, and improving its model representations in tropical and/or sub-tropical savannas. The phenology model in SiB is tested and developed to better represent seasonal cycle of greening. Instead of using water vapor deficit as a proxy for available water, soil moisture is employed to calculate onset of greening season for grass. The study is based on observations collected at South Africa savanna site and performed by running multiple year phenology model simulations. Observed and modeled fluxes of latent and sensible heat, as well as net ecosystem exchange, at this and other 6 locations are used for evaluation.

CHAPTER 2 Data And Model Description

2.1 Model description

2.1.1 The Simple Biosphere Model (SiB)

The Simple Biosphere Model (SiB) was introduced in 1986 by *Sellers et al.* (1986) with the intent to be used as a lower boundary condition for Atmospheric General Circulation Models. SiB simulates the processes that control the exchange of mass, energy, momentum, and trace gases between the atmosphere and terrestrial biosphere and was developed to provide a valuable modeling function for meteorologists and ecologists alike.

A second version of the model (SiB2) was released in 1996 (*Sellers et al.* (1996a)). Canopy representation was bolstered with improved stomatal physics (*Sellers et al.*, 1992; *Collatz et al.*, 1991; *Sellers* 1987) and inclusion of the C4 photosynthetic pathway following *Collatz et al.*, (1992). Vegetation phenology, previously determined by lookup table, was prescribed from satellite-observed phenology using Normalized Difference Vegetation Index (NDVI) information (*Sellers et al.*, 1996b).

A revised model based on SiB2 has been developed in order to improve the accuracy of the description of energy and the water budget between land-surface and atmosphere. This new version of the Simple Biosphere Model is called version 3.0 (hereafter SiB3) and it the one used in this study.

A brief description of model's essentials is provided below, while an in-depth model description can be found in *Sellers et al.*, 1986, *Sellers et al.*, 1996 a and b, *Randall et al.*,

1996 and Baker 2003, 2008.

Before proceeding, terms used in this study such as water vapor pressure deficit (*vpd*) and plant available water (*pawfrac*) fraction are defined more precisely.

Plant available water (PAW) is the water available to plants for root uptake, and is defined as the difference between the soil's volumetric water content (VWC) and wilt point (the lowest water content at which plant can extract moisture by its roots). Since the maximum VWC is controlled by soil porosity we can write:

$$paw_{max} = P - \theta_{wp}$$

where *P* is the porosity (determined based on the percent sand and clay), and θ_{wp} is the VWC at wilt point. *Pawfrac* is simply defined as a ratio between current and maximum PAW:

$$pawfrac = paw / paw_{max}$$

Or in other words, *pawfrac* is a defined by both plants ability to extract the moisture (highly dependent on root fraction) from the soil and soil's ability to store/hold the moisture (porosity).

SiB3's field capacity and wilt point are calculated using a relationship between soil water potential and volumetric water content (Clapp and Hornberger, 1978). The percent of sand and clay is found following pedo-transfer regression equations provided by Cosby et al. (1984). Gravitational drainage is accounted by using Darcy's Law, and the change in soil moisture with time (in each layer) is solved by using the Richard's equation. Details on this are given in Harper (2011).

Vapor Pressure Deficit, or *VPD*, is the difference (deficit) between the amount of moisture in the air and how much moisture the air can hold when it is saturated:

$$vpd = e_{sat} - e$$

where e_{sat} and e are saturated vapor pressure and current vapor pressure, respectively.

Therefore, a relative humidity of 100% corresponds to *vpd* of zero.

Five major improvements in SiB3 (see Fig. 2) compared to SiB2 are made:

- The original three soil layer structure has been modified to 10 soil layer structure, 3.5 meter deep. With an increased number of soil layers and a revision of the soil's structure, the model has become more favorable to water storage and also gained a more realistic account of water transportation throughout the soil layers (Fig. 2). This was adapted from the Community Land Model (Dai et al. 2003) and based on the earlier NCAR Land Surface Model (Bonan 1996).

- Instead of a three-layer model in which roots are simply pooled into the second layer, SiB3 projects adjusted water extraction root profile throughout all the layers. The advantage of including root distribution analysis is that the model allows for a more realistic hydrological process in soil layers, especially vertical water transportation through soil layers.

- Plant available water (PAW) has replaced root zone water to be used in the calculation of the water stress factor. Soil moisture stress is calculated layer-by-layer and is weighted by the fractional amount of roots in each layer. This method is a simple but plausible way to deal with the entire plant-soil system and have provided a foundation for this research.

- Prognostic temperature, water vapor, CO₂, heat and water fluxes are introduced in “canopy air space” storage, and predicted from one time step to another (Baker 2008).
- Snow structure and a multi-layer soil model based on CLM (Dai *et al.*, 2003) have been applied in the model, bringing also a more realistic assessment of the soil’s hydrological process.

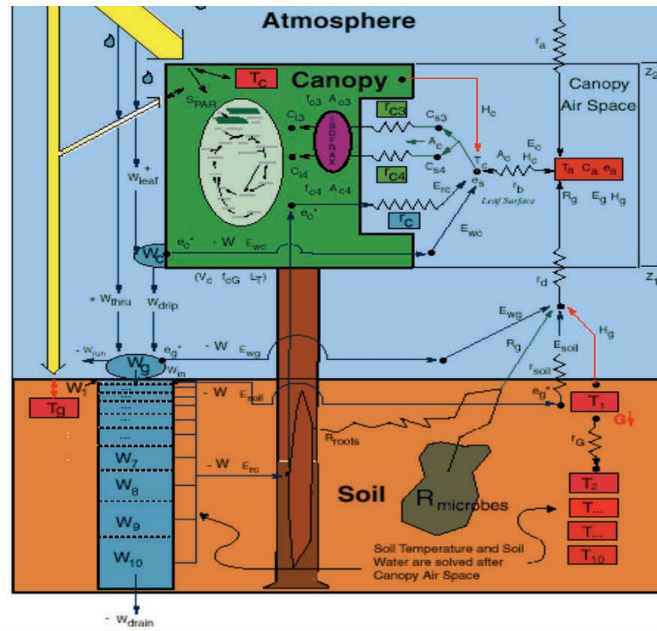


Figure 2 Schematic Simple Biosphere Model, version 3 (SiB3)

Since the soil moisture variability leads to a clear and wide variation in seasonal climate variability (Douville 2003) and is essential for the results presented in this work, it is important to completely understand its role and representation in the model and model’s land-atmosphere interaction.

a) First, soil moisture in the model is affected by precipitation. Two elements of precipitation are described in the model: a convective component and a grid area component. The former presents the shower-type locally precipitation, which will run off much faster than the grid area precipitation, which is more uniform, and has larger scale.

b) Second, the root distribution throughout the entire soil also makes impacts on variation of soil moisture. SiB2, a three-layer model is employed. The upper layer is a thin layer, from which water evaporates into the atmosphere directly once the pores of the soil are at or near saturation. The second layer is the root zone, where all roots of plants are located. Beneath the root zone, there is an underlying recharge layer, where the transfer of water is governed only by the gravitational drainage and hydraulic diffusion. In SiB3, a ten-layer model is employed and based on Jackson et. al (1996) plant roots are considered exponentially distributed throughout the whole soil layers.

c) Finally, the variability of soil texture is one of the key elements that influence soil moisture with soil texture used to describe soil types by how much sand, silt and clay are present, including information on ability of different types of soils to hold water.

Overall, SiB3 can be described as a land surface model that directly addresses the effect of vegetation on the interaction between the land surface and the atmosphere by modeling the physiological and biophysical processes influencing radiation, momentum, mass, and heat transfer (Sellers et al., 1997). For purposes of this research it is also important to note that SiB3's modeled fluxes of heat and water vapor are dependent not only on meteorological drivers (temperature, humidity, wind, and precipitation) but are also highly dependent on the characteristics of the canopy vegetation and soil type. SiB3 specifies these vegetation and soil parameters as monthly values interpolated daily, based on vegetation type (see Fig. 3). The parameters are specified using a combination of land cover type (Hansen et al., 2000), monthly maximum normalized difference vegetation index (NDVI) derived from advanced very high-resolution radiometer (AVHRR) data (Tucker et al., 2005), and soil properties observed in the area (Silver et al., 2000). Time-invariant

vegetation biophysical parameters such as canopy height, leaf angle distribution, leaf transmittance, and parameters related to photosynthesis are based on values recorded in the literature and assigned via look-up tables (Sellers et al., 1996b). In this study a phenology model (described below) replaces all aforementioned.

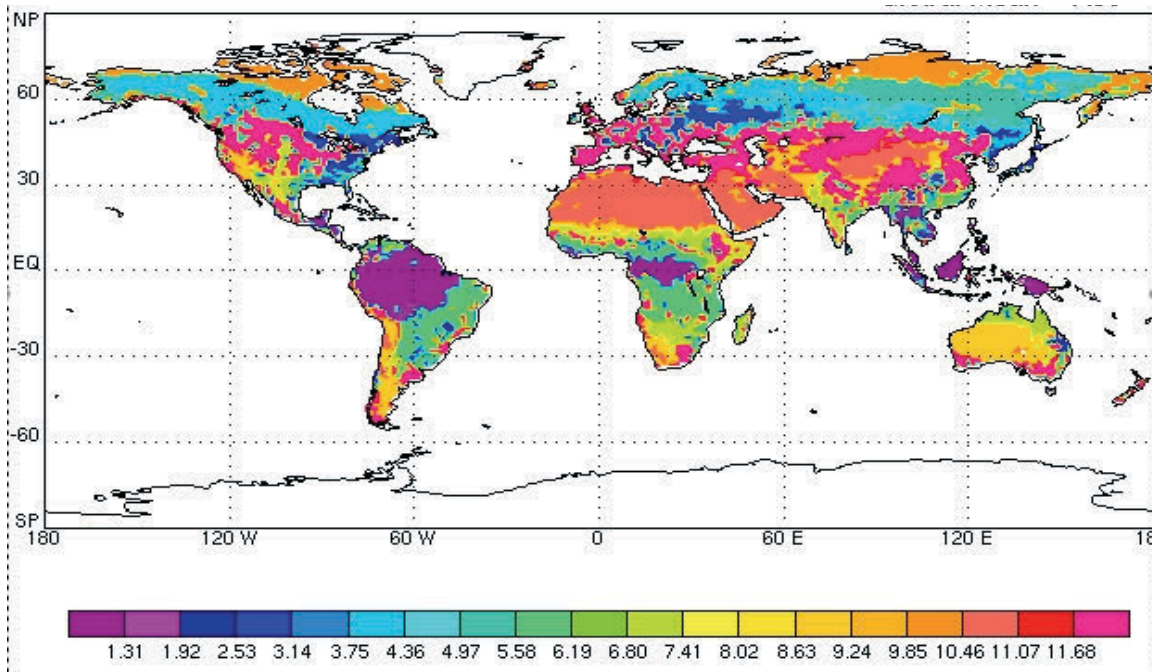


Figure 3 Spatial distribution of different vegetation in SiB model: 1- Broadleaf evergreen; 2- Deciduous Broadleaf Trees; 3- Mixed forest; 4- Needleleaf/pine tree; 5- Needleleaf deciduous; 6- Broadleaf with ground cover; 7- Ground cover/maize optical; 8 - Not used; 9 - Shrubs; 10 - Tundra; 11 - Low-latitude desert; 12- Crop

Two modifications, however, are made to the SiB3 code for this study purposes. First is the change in the manner in which the plant available water fraction, *pawfrac*, is calculated. As mentioned above, in SiB3, *pawfrac* is calculated through all 10 soil layers as the ratio of the available amount of water in all 10 layers to the maximum amount of water that those 10 layers can hold. At the same time roots are distributed exponentially through the column, dependent on the biome type as described in Jackson et al. (1996) and Canadell et al. (1996). This allows consideration of the entire column when calculating soil water stress on photosynthesis. However, in this study *pawfrac* is calculated using only the layers

where plant roots are present, ignoring the others, since plants do not make any use of moisture from those. Also, the contribution of layer moisture to the *pawfrac* value is related directly to root fraction of a given layer, meaning that layers with higher root fractions will contribute more to the *pawfrac* value. This provides a more realistic representation of the amount of water available to the plant. This works well for grasses. However, it is unrealistic for tropical forest as explained in Baker (2008). The second change is in the amount of water required to saturate the soil. This value is set to what it used to be in SiB2 as explained by Sellers (1985) and is found to be better in describing the soil properties at grasslands. This change prevented the soil from being dry for unrealistically long, or saturated for unrealistically short time intervals.

2.1.2 Phenology model

The Simple Biosphere Model (SiB3), driven by biophysical parameters derived from Prognostic Phenology model (Stöckli et al. 2008, 2011), is used in this study. The Growing Season Index (GSI) by Jolly et al. (2005) diagnoses the state of vegetation by use of three major climatic drivers serving as surrogates for the underlying controls on vegetation phenology: low temperatures, evaporative demand, and photoperiod. Stöckli et al. (2008b) and this study extended the GSI model into a prognostic phenology model that predicts the biophysical vegetation states of fraction of photosynthetically active radiation (FPAR) and Leaf Area Index (LAI). Detailed model description can be found in Stöckli et al. (2011). Essentials are outlined below.

The product of three environmental factors $f(T)$, $f(L)$ and $(1-f(W))$ form the GSI:

$$GSI = f(T) \cdot f(L) \cdot (1 - f(W)) \quad (1)$$

where factors are given by:

$$f(x) = \begin{cases} 0 & \text{if } x(t) \leq x_{\min} \\ \frac{x(t) - x_{\min}}{x_{\max} - x_{\min}} & \text{if } x_{\min} < x(t) < x_{\max}, \\ 1 & \text{if } x(t) \geq x_{\max} \end{cases} \quad (2)$$

where t refers to time and x defines temperature (T), light (L) and moisture (W). In the phenology model these values are represented by multiday running mean averages of the minimum daily temperature, the mean daily radiation¹ and the mean daily vapor pressure deficit, respectively, calculated using assigned averaging times. In Eq. (2) x_{\max} and x_{\min} are predefined, constant maxima and minima of T, L and W.

The prognostic phenological state P can be related to the biophysical state FPAR by use of a linear relationship (Sellers et al., 1996a; Los et al., 2000),

$$P = f(FPAR) \quad (3)$$

where $f(x)$ is given in equation (2), $FPAR_{\min}$ and $FPAR_{\max}$ are the minimum and maximum FPAR corresponding to the least and most developed state of vegetation.

¹ The mean of the direct and diffuse radiation components (both longwave and shortwave) reaching the surface

The growth vector $\partial GSI/\partial t$ then gives the direction and rate of leaf growth or decay used to calculate the change in FPAR with a logistic growth model,

$$\frac{\partial GSI}{\partial t} = GSI - P \quad (4)$$

$$\frac{\partial FPAR}{\partial t} = \gamma \cdot \frac{\partial GSI}{\partial t} \cdot P(1-P) \quad (5)$$

As presented by Dickinson et al. (2008), growth and senescence can be modeled as two separate processes. Stöckli et al. (2011) choose a different maximum rate for leaf growth γ_g (day^{-1}) and leaf senescence (γ_d) instead,

$$\gamma = \begin{cases} \gamma_g & \text{if } \partial GSI \geq 0 \\ \gamma_d & \text{if } \partial GSI < 0 \end{cases} \quad (6)$$

According to Sellers et al. (1996a) and Los et al. (2000), the biophysical state LAI (m^2m^{-2}) can be related to FPAR by use of the Monsi-Saeki light interception model

based on Beer's law for LAI, respectively (Monsi and Saeki, 2005),

$$\frac{\partial LAI}{\partial t} = \frac{\partial LAI}{\partial FPAR} \cdot \frac{\partial FPAR}{\partial t} \quad (7)$$

$$LAI = \frac{\ln(1 - FPAR / f_v)}{\ln(1 - FPAR_{sat})} LAI_{\max f_v} \quad (8)$$

where f_v is the vegetation fraction, and $FPAR_{sat}$ is the FPAR value reached at the maximum leaf area index LAI_{\max} ($m^2 m^{-2}$).

2.2 Data

Data used in this study are obtained mainly by direct tower-mounted instruments (Baldocchi, et al. 2001) at 7 different locations spread over three continents (Africa and North and South America). The towers at these locations were, or still are, parts of observational sites of flux network or of a specific field campaign. Location and climate description at each of the sites is given below. Site S0 is used in this study to develop methodology, while sites S1-S6 are used to test its robustness and to learn more about its applications at different climates than one seen at S0. Locations and site names, together with their abbreviations are given in Fig. 4 and Table 1.



Figure 4 Measurements site locations

2.2.1 Site descriptions

Table 1 Measurements site abbreviations, locations, and principal investigators.

Site	Site Name and Abbreviation	Latitude (°)	Longitude (°)	Elevation (m)	PI
S0	Skukuza ZA-KRU	-25.0197	31.4969	357	Robert Scholes
S1	Lethbridge CA-Let	49.7092	-112.9403	951	Lawrence Flanagan
S2	Shidler Tallgrass Prairie US-Shd	36.9333	-96.6833	346	Shashi B. Verma
S3	Fermi Prairie US-IB2	41.8406	-88.2410	226	David R. Cook Roser Matamala
S4	Vaira Ranch US-Var	38.4067	-120.9507	129	Dennis D. Baldocchi
S5	Fort Peck US-FPe	48.3077	-105.1019	634	Tilden P. Meyers
S6	Fazenda Nossa Senhora LBA -FNS	-10.77402	-62.33741	293	Antonio Ocimar Manzi

S0 – Skukuza, Kruger Park, South Africa

Approximately 5 years of data from South Africa, Kruger National Park, flux tower site in Skukuza (Fig. 6) is used as driver data for SiB. The Skukuza site is located at 357 m above sea level, receives 550 ± 160 mm of rainfall annually, with about 65 rainy days per year, almost entirely between November and April. The year is divided into a warmer, occasionally wet growing season and a warm, dry non-growing season. The site is unique in that the micrometeorological instruments are positioned on a tower located between two distinct savanna types, a broad-leaved *Combretum* savanna and fine-leaved *Acacia* savanna. These contrasting savanna types are found on soils of differing texture, water holding capacity and nutrient status, and are characterized by different physical structure, physiology and phenology. Wind directions are such that obtaining a good sample of net

ecosystem fluxes from both ecosystems is expected. Williams et al. 2009 provides detailed description of the site and measurements.

S1 - Lethbridge, Canada

The site was established in June 1998, and is an associated site in the Fluxnet-Canada and Canadian Carbon Program research networks. It covers 64 ha and is located just west of the city limits of Lethbridge, Alberta, Canada (Lat. 49.470919°N; Lon. 112.94025°W; Elev. 951 m). The site is in the northwestern short/mixed grassland eco-region of the Great Plains, which is the second largest ecozone in North America and covers approximately $2.6 \times 10^6 \text{ km}^2$ (Ostlie et al., 1997; Savage, 2004). The climate in this region of the Great Plains is semi-arid continental and the mean daily temperatures (1971–2000) for January and July, measured at the Lethbridge airport, are -7.8 °C and 18.0 °C, respectively (Environment Canada, 2010a). The Lethbridge airport is located only 14 km from the site. Mean annual precipitation (1971–2000) is 386.3 mm, with 30% falling in May and June. Average pan evaporation (Class A) exceeds the average precipitation by at least 200% and often 300% during the summer months (Flanagan and Johnson, 2005). The study area is very flat and the soil (orthic dark-brown chernozem; Agriculture Canada, 1987; Flanagan and Johnson, 2005) was underlain by a thick glacial till with very low permeability and no water table (Scracek, 1993; Berg, 1997). An in detail soil description, which is mainly clay loam (28.8% sand, 40% silt, 31.2% clay) can be found in Flanagan and Johnson 2005. The plant community at the site was dominated by the grasses *Agropyron dasystachyum* [(Hook.) Scrib.] and *Agropyron smithii* (Rydb.) (Carlson, 2000; Flanagan and Johnson, 2005). Other plant species present included: *Vicia americana* (Nutt.), *Artemesia frigida* (Willd.), *Koeleria cristata* [(L.) Pers.], *Carex filifolia* (Nutt.), *Stipa comata* (Trin. and Rupr.), *Stipa viridula*

(Trin.). The average (- SD) canopy height from 2001 to 2006 was 31.7 - 7.4 cm, and it ranged from 18.5 - 3.4cm in 2001, which was a very dry year, to 34.3 - 9.5 cm in 2002, a relatively wet year. Flanagan and Adkinson (2011) provide detailed description of the site and measurements.

Meteorological instrumentation to monitor environmental conditions has operated continuously at the site since it was established in 1998, and has been described in detail previously (Flanagan et al., 2002; Wever et al., 2002).

S2 - Shidler Tallgrass Prairie, Oklahoma, US

Measurements were made at a native tallgrass prairie site ($36^{\circ}56'N$; $96^{\circ}41'W$) near Shidler, OK, USA during 1997–2000 period. This area is Bluestem Prairie typical to central Kansas and northern Oklahoma. The vegetation is dominated by warm season C₄ grasses (e.g. *Schizachyrium scoparium* (Michx.) Nash, *Bouteloua gracilis* (H.B.K) Lag. Ex Steud, *Andropogon gerardii* Vitman, and *Sorghastrum nutans* (L.) Nash). The soil is a silty clay loam of Wolco-Dwight complex (thermic Pachic Argiustolls and mesic Typic Natrustolls) with heavy clay starting at depths between 0.2 and 0.5 m. The soil is underlined with a limestone bedrock at depths of 0.2–1.5 m, occasionally surfacing in the western and eastern parts of the site. The prairie was burned in the spring of each year (March 28, 1997; March 31, 1998; April 6, 1999; and March 28, 2000). The prairie was not grazed during the measurement period.

More details of the measurements and calculations are given in Suyker and Verma 2001.

S3 - Fermi Prairie, Illinois, US

The site is a restored tallgrass prairie located at the Fermi National Accelerator Laboratory (Batavia, IL, USA). The site had been cultivated for over 100 years before it was restored to prairie in 1990 using native tallgrass prairie vegetation (Betz, 1986; Betz *et al.*, 1996; Matamala *et al.*, 2008). At the time of the study, dominant vegetation consisted of native and nonnative C₃ forbs and grasses with some contribution of C₄ grasses. The site topography has gradual variations in elevation of less than 3 m. Soils are predominantly silty loams and silty clay loams belonging to the Mundelein soil series. The prairie is burned biannually; during the study it was burned in the spring of 2009.

The site contributes to the AmeriFlux network (site US-IB2), and calibration of instruments and data handling were in accordance with AmeriFlux standards. Zhang *et al.* (2007) and Gomez-Casanovas *et al.* (2012) provide detailed description of the site and measurements.

S4 - Vaira Ranch, California, US

The site is a grazed grassland opening in a region of oak/grass woodland. It was established in October 2000 as part of the AmeriFlux network (Law *et al.*, 2003). It is located on the foothills of the Sierra Nevada Mountains, and is about 35 km southeast of Sacramento (38°24.400'N, 120°57.044' W, and 129 m a.s.l.).

The soil is a very rocky silt loam (Lithic xerorthents). It contains 30% sand, 57% silt and 13% clay. Its bulk density at surface layer (0–30cm) is around $1.43 \pm 0.10 \text{ g cm}^{-3}$. Total nitrogen and carbon content of the soil were about 0.14 and 1.39%, respectively. The soil profile is about 0.5m deep, and overlays fractured rock.

The climate at the site is Mediterranean type with clear days, high temperatures, and virtually no rainfall during the summer. In contrast, the winter is relatively cold and wet. The mean annual temperature was 16.2 °C during 2001 and 566 mm of precipitation fell. These values are close to climatic means, determined over 30 years from a nearby weather station at Ione, CA (mean air temperature is 16.3 °C and mean precipitation is 559 mm).

The grassland is dominated by cool-season C3 annual species. More than 95% of species composition at the site, are *Brachypodium distachyon* L., *Hypochaeris glabra* L., *Trifolium dubium* Sibth., *Trifolium hirtum* All., *Dichelostemma volubile* A., and *Erodium botrys* Cav. The maximum grass height in the peak growth period (late April to early May) could reach up to 0.55 ± 0.12 m.

Xu and Baldocchi (2004) provide detailed description of the site and measurements.

S5 - Fort Peck, Montana, US

The study area focuses on AmeriFlux tower site located outside of Fort Peck ($48^{\circ} 18' 36''$, $105^{\circ} 06' 00''$, elevation = 634 m a.s.l.) in the northeast corner of Montana. The tower itself is situated in a grazed grassland along the Poplar River, but the Landsat scene also contains a significant fraction of rainfed and irrigated agricultural fields. The topography is predominantly flat, and there are several lakes and reservoirs contained within the scene. Soils around the site are moderately drained clay loams. See Wilson and Meyers (2007) for further details on the Fort Peck AmeriFlux site.

The grassland site in Fort Peck undergoes seasonal winter conditions. The Fort Peck site has been operating since 2000. It is 48 km east of Wolf Point, MT, about 72 km from the Canadian border, and located in a grazing area of the Great Rolling Plains Grasslands. The

soils consist of deep, moderately drained clay loams and the soil surface shows evidence of a large excess of precipitated calcium carbonate. The average annual precipitation is about 100 mm during winter months from November to April, and roughly 200 mm rainfall is received during the growing season, which is freeze-free and often runs from May to September.

Schmidt et al. (2011) provide detailed description of the site and measurements.

S6 - Fazenda Nossa Senhora, Brazil

This site ($10^{\circ} 45'S$, $62^{\circ} 22'W$) was established in October 1991 on a cattle ranch 220 m above sea level about 50 km east-north-east of Ji-Parana. The site was deforested in about 1977 and is in the center of an area of about 50 km in radius which has been largely cleared. The grass (*Brachiaria brizantha*) is clumpy and the original planting rows can still be clearly seen from above (see McWilliam et al. (1996) and Roberts et al. (1996)). The area of bare soil was surveyed in April 1993 and found to form 12% of the surface area. The ranchland has several palms with very few dead tree trunks. The pasture had been burnt in the month prior to equipment installation, but it was not burnt again during the measurements. The automatic weather station was installed at the site.

Andreae et al. (2002) provide detailed description of the site and measurements.

2.2.2 Tower data

At the Skukuza site (S0) a 22-m tower was instrumented at 16 m with a sonic anemometer (Gill Instruments Solent R3, Hampshire, England) measuring three-dimensional, orthogonal components of velocity (u , v , w ; $m s^{-1}$) as well as the “sonic” air

temperature (T_a ; °C), and a closed-path infrared gas analyzer (IRGA; LiCor 6262; LiCor, Lincoln, Neb.) measuring concentrations of water vapor (q ; mmol H₂O mol⁻¹ moist air), and CO₂ (μmol CO₂ mol⁻¹ air). Manual IRGA calibrations were performed approximately monthly. Calibrations were done in the field using Level-5 (99.999% pure) N₂ for CO₂ and H₂O zero (this was also the reference gas running continuously through the reference cell in the 6262). Spans were carried out using National Oceanographic and Atmospheric Administration (NOAA) secondary standard calibration gases calibrated to <0.2 p.p.m. for CO₂ and a LiCor dew point generator for H₂O. Analytical flux footprint estimation (Gash 1986; Hsieh et al. 2000) indicates that a source area within 130 m upwind of the tower typically contributes 90% of the measured flux, and a source area within 1.3 km contributes 99% of the flux.

The flux and state observations from this site analyzed in this study were taken between March 2000 and November 2005. All measurements are available at 30min temporal resolution. Fires burned the area in both 2000 and 2001 dry seasons (fractional burn of the herbaceous ground cover was near 100%), resulting in relatively long periods of measurements that are either missing or classified as missing. Substantial amounts of data are missing in latter years as well (see Fig. 6). In order to make a continuous data set, for SiB's meteorology driver purposes, interpolation of the closest valid measurements is used at times when data are missing. These variable are denoted in third column of Table 1 as 'SiB3'. For longer periods of missing data for variables with diurnal or seasonal cycle, climatological mean obtained from valid data is used. Missing rain is replaced with zero values at all times. Validation results are based on comparing the measurements to the

results only at those times when measurements were available; no interpolation was done for these purposes.

Data are collected in similar manner at all other six sites. Table 1 lists measured variables used in this study, together with their original units and what the data are used for.

Table 2 Skukuza tower data used in the study; original units (as provided from the site); what the data are used for

Variable	Units	Use
Temperature	K	SiB3
Specific humidity	g kg ⁻¹	SiB3
Long wave incoming radiation	W m ⁻²	SiB3
Short wave incoming radiation	W m ⁻²	SiB3
Rainfall amount	mm 30min ⁻¹	SiB3
Latent heat flux	W m ⁻²	Evaluation
Sensible heat flux	W m ⁻²	Evaluation
Turbulent CO ₂ flux	mg CO ₂ m ⁻² s ⁻¹	Evaluation
16 cm soil temperature	C	Verification

CHAPTER 3 Methodology

Ecosystem water use, productivity, and respiration all respond to the episodic availability of water (Austin et al. 2004; Baldocchi et al. 2006; Huxman et al. 2004; Jenerette et al. 2008; Porporato et al. 2001; Rodriguez-Iturbe et al. 1999; Xu et al. 2004). Many processes in arid and semi-arid ecosystems are dormant until activated by a pulse of rainfall, and then decay from a maximum rate as the soil dries. Respiration responds to wetting within days, while photosynthesis takes a week or longer to reach its peak if the rainfall was preceded by a long dry spell (Williams 2009). The ability of models to timely capture the onset of greening season is essential for successful simulation of ecosystem behavior.

This Chapter explains the challenges of calculating LAI value and its dependence on soil moisture and other factors. Results presented here are extended in Chapter 4 to give a full understanding of their role in the forecasting of LAI process.

3.1 Detection of the start and end of greening season

As addressed in Chapter 1 a Start Of the Season (SOS) of any biome depends mostly on three conditions: light, temperature and moisture. SOS occurs when these conditions first time become preferable for plant growth. For grasslands in tropics, subtropics and Mediterranean-like climates, moisture is usually the only factor that really constrains greening since light and temperature are sufficient year-round.

A current phenology model (i.e. Stöckli 2008, 2011) clearly reflects oscillation of leaf area index (LAI) through the growing season index (GSI), which is a function of the three

variables listed above. As an illustration, in Fig. 5 are shown the values for each of the three contributors of GSI at Skukuza site for time period of one year.

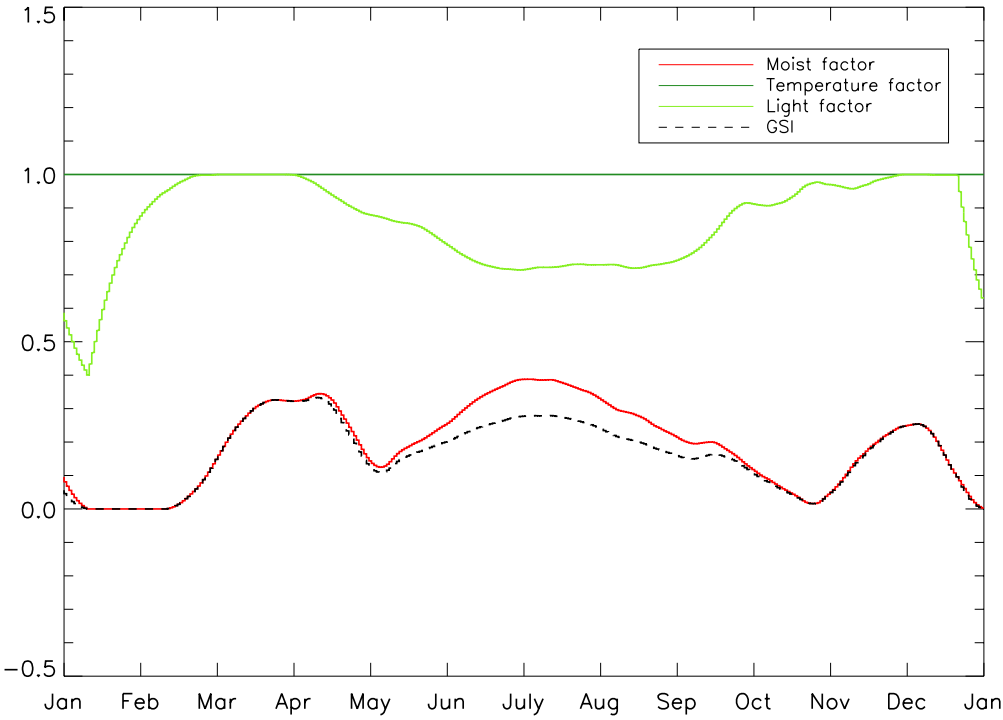


Figure 5 Change in GSI 10-day running mean contributors at Skukuza site in year 2002.

Temperature (T) and light (L) factors are close to the value of 1 during most of the year. The dip in the light factor curve at the beginning and at the end of the year is due to the increased cloudiness during wet season at Skukuza (approximately November to March) while temperature factor is equal to 1 all the time. This means that heat and light are not limiting factors for GSI. The moist factor governs the behavior of GSI.

The GSI curve in Fig. 5 is obtained by using water vapor pressure deficit to calculate the moist factor, the third term on the right hand side of Eq. (1). Since moisture governs GSI one would expect to see the GSI curve reaching high values during wet season (Nov-March) and low values during dry season (May-Oct). This, however, is not the case. Apparently, at Skukuza site water vapor deficit change is not primarily related to the raining events but

rather to its advection or boundary layer depth and perturbations. In other words, the fact that water vapor pressure deficit is low, depicting moist air, does not necessarily relate to sufficient amount of moisture being available to the plants. Plants, or in this case grass, are making the use of water exclusively through the roots from the soil. Water vapor deficit depicts not soil but air condition, having sometimes little or even nothing to do with the amount of moisture available to plants. A simple change in planetary boundary layer depth, caused for example by large-scale circulations, may result in air moisture inflow from neighboring moist regions making no changes to the soil water content but erroneously implying an increase in GSI value even for periods when no rain is seen and all vegetation is brown.

To quantify the threshold value of plant-available water, a clear condition for SOS and the end of season (EOS) is necessary. This may be especially important in warm subtropical and Mediterranean-like regions, with sufficient amount of light, with the rainfall condition likely being a dominant factor (Williams et al. 2009).

3.2 New methodology for calculating Growing Season Index (GSI)

The importance of correct GSI presentation in model simulations of LAI has already been addressed. Here we focus on GSI calculations and describe in detail how the new method is being implemented, providing step-by-step description of all the changes made to the phenology model that is currently being used.

The Growing Season Index (GSI) and Leaf Area Index (LAI) are given by Equations (1)-(8). In current version of phenology model (Section 2.1.2 - Stöckli et al. 2008, 2011) the moist factor, defined as $1-f(W)$ in Eq. (1), was a function of atmospheric water vapor

pressure deficit (vpd). However, this is far from how the plant growth in nature depends on moisture supply. Plants employ roots in process of extracting available moisture from the soil and therefore, soil moisture is a choice that should be more suitable than vpd as an indicator of plant growth. This should be most obvious in rain-driven vegetation such as tropical grasslands, a biome this study is focused on. In the mid- and high latitudes phenology is controlled mostly by temperature and photoperiod (Myneni et al., 1997; White et al., 1997; Chuine and Cour, 1999; Jarvis and Linder, 2000; Schwartz and Reiter, 2000), while in the tropics phenology is controlled either by rainfall (Childe, 1989; de Bie et al., 1998; Bach, 2002) or photoperiod (Njoku, 1958; Borchert and Rivera, 2001).

Scholes and Walker (1993) and Williams and Albertson (2004) suggest that using *soil* conditions rather than atmospheric conditions may be better approach for defining GSI at these sites. Therefore we introduce new definition for GSI as

$$GSI = f(T) \ f(L) \ g(W) \quad (9)$$

where $g(W)$ represents the available moisture for plant rather than moisture deficit as in Stöckli al. 2008 (e.g. Eq. (1)). A desired characteristic of $g(W)$ with respect to rain-driven vegetation is a capability of recognizing greening season as a period

when moisture is sufficient to support plant grow. To reflect this we define g as:

$$g(x) = \begin{cases} 0 & \text{if } x(t) \leq x_{\min}(t) \\ \frac{x(t) - x_{\min}(t)}{x_{\max}(t) - x_{\min}(t)} & \text{if } x_{\min}(t) < x(t) < x_{\max}(t), \\ 1 & \text{if } x(t) \geq x_{\max}(t) \end{cases} \quad (10)$$

Note that this formula is similar to Eq. (2), however it includes time dependent minima and maxima used to provide correct detection of SOS and EOS. For example, if defined as fixed values, the length of greening season could be overestimated or underestimated due to incorrect detection of SOS. This becomes obvious in years of drought, as drought is characterized by an extended period of below average precipitation. In that situation, soil moisture values could drop below values characteristic for wet years. At that point, even precipitation that would trigger plant growth under regular conditions may not be sufficient to boost the soil moisture back into its typical range. Therefore, if fixed soil moisture minima are used to define the period of growing, as in Eq. (2), it will result in no detection of SOS as long as drought conditions are present. Similarly, fixed value of maxima may not reflect the nature of the plant to start drying its leaves after prolonged periods without rain if soil moisture is relatively high (i.e. higher than the maxima). In essence, time dependence of minima and maxima introduces the plant's natural sensitivity not only to soil moisture, but also to its change.

As in Stöckli (2008) we define x as a moving average:

$$x^t = \alpha \cdot x^{t-1} + (1 - \alpha) \cdot y \quad (11)$$

where y is a current (observed) value. The coefficient α is:

$$\alpha = \exp\left(-\frac{1}{z_{pft}}\right) \quad (12)$$

where z_{pft} is a time averaging factor dependent on plant functional type pft . We similarly define x_{\min} and x_{\max} , however with different time averaging factors.

A SiB variable that is considered most adequate in representing the soil moisture conditions relative to the plant is plant available water fraction (*pawfrac*). According to its definition (Chapter 1) *pawfrac* reflects soil moisture that is available to the plant through all soil layers in which the roots are present. The seasonal cycle of *pawfrac* provides wet and dry season contrast in LAI value, while intra-seasonal oscillation is achieved by using adjustable minima and maxima of *pawfrac* in Eq. (10).

To ensure the complete understanding of all changes the implementation of the new method requires, some of Eqs. (2) through (10) are repeated below in the form as they are used in the proposed method.

Since $pawfrac$ is chosen for representing the moisture factor in Eq. (9). The function g is:

$$g=g(W=pawfrac)$$

with $g(W=pawfrac)$ given by Eq. (10) and x equal to $pawfrac$. Therefore, from Eq. (10) we get:

$$g = \begin{cases} 0 & \text{if } \dots \\ \frac{pawfrac(t) - pawfrac_{\min}(t)}{pawfrac_{\max}(t) - pawfrac_{\min}(t)} & \text{if } \dots \\ 1 & \text{if } \dots \end{cases} \quad (13)$$

... $pawfrac(t) \leq pawfrac_{\min}(t)$
 ... $pawfrac_{\min}(t) < pawfrac(t) < pawfrac_{\max}(t)$
 ... $pawfrac(t) \geq pawfrac_{\max}(t)$

with $pawfrac$ at time step T:

$$pawfrac^T = \alpha \cdot pawfrac^{T-1} + (1 - \alpha) \cdot pawfrac_{state} \quad (14)$$

Here, the current time step $pawfrac^T$ is a combination of the previous $pawfrac^{T-1}$ value and a current predicted $pawfrac_{state}$ value both weighted by a 21-day mean in Eq. (12).

Similarly, the minima and maxima in Eq. (13) at each time step are calculated as:

$$pawfrac_{\min}^T(t) = \beta \cdot pawfrac_{\min}^{T-1}(t) + (1 - \beta) \cdot pawfrac_{lower} \quad (15)$$

$$pawfrac_{\max}^T(t) = \beta \cdot pawfrac_{\max}^{T-1}(t) + (1 - \beta) \cdot pawfrac_{upper} \quad (16)$$

where all symbols are as already explained, except that now the weight β denotes a different time averaging interval reflecting the length of dry season. The terms $pawfrac_{lower}$ and $pawfrac_{upper}$ are given by:

$$pawfrac_{upper} = pawfrac^{T-1} \cdot (1 + eps_{upper}) \quad (17)$$

$$pawfrac_{lower} = pawfrac^{T-1} \cdot (1 - eps_{lower}) \quad (18)$$

where eps_{lower} and eps_{upper} are empirical limits used to define the distance between current $pawfrac$ value and its current minima and maxima. These values allow adjustments of moving minima and maxima, they are pre-defined in such way to correspond to the strength of the contrast of the soil moisture content between dry and wet seasons. In this study it is empirically found that $eps_{lower}=0.4$ and $eps_{upper}=0.1$ best describe those contrasts except for site S6 where $eps_{lower}=0.2$.

The methodology presented above is most suitable for vegetation that is rain-driven, such as C4 grass. Complete lists of vegetation types and distributions are given in Appendix B. Other vegetation (e.g. trees, evergreen type of vegetation and to some extent shrubs)

tends to be not so strongly rain dependent when it comes to the initiation of green season and the original, Stöckli's method, which suggests using a water vapor pressure deficit approach, is found to be equally good. However, despite the vegetation type, all plants depend on soil- rather than the air- moisture, thus, the proposed methodology is a step closer to correct representation of the plant's nature and should be capable of replacing the existing method without any drawbacks.

3.3 Evaluation

With very few direct LAI measurements and all known issues of MODIS² LAI estimates (Sea et al. 2011), results are evaluated by comparison of observed and modeled fluxes of carbon and latent (LH) and sensible heat (SH). Skukuza tower and six other site measurements of these three fluxes are available at 30-60min temporal resolution and easily comparable to their values in SiB's standard output. Comparing measured and calculated fluxes provides an excellent tool for evolution of the results and comparison of the methods described above. Since the amount of green vegetation strongly influences all of the three fluxes any unrealistic variation of prognostic LAI value would be reflected through the changes in either of them.

² Moderate-resolution Imaging Spectroradiometer

CHAPTER 4 Results and Discussion

The goal of this study was to provide a potential improvement in SiB's forecasting of seasonal change in LAI in a rain-driven biomes. For this purpose a new, *pawfrac-method*, which links plant available soil moisture to the greening of plants and production of leaves, is developed and implemented into the phenology code. To be successful, the *new method* must provide a foundation for forecasting that is better than the one currently being used. Since the current method uses water vapor pressure deficit as governing parameter, these simulations are used to define a baseline against which improvements can be gauged. Therefore, for the compression purposes before *pawfrac-method* results are presented, current *vpd-method* results are shown. Analyses are performed at Skukuza (S0) site while other sites' results are presented in evaluation section at the end of this chapter. Before any of findings are discussed, it is necessary to test our ability to detect beginning and end of greening season at rain-driven biomes and then investigate if our findings support the idea by Archibald and Scholes (2007) of using the soil moisture information in predicting the greening seasonality of vegetation.

4.1 Detection of greening season

Based on Ati et al. (2002) a criterion for initiation of greening season is found to be given by the first occurrence of a 10-day running mean of temperature above 23.5 °C and a 10-day running mean of 30min rainfall accumulation of more than 0.05 mm between October 1st and December 31st. Similarly, an end of season (EOS) criterion is found to be: the first day between March 1st and July 1st when the 10-day running mean temperature is below 23.5 °C and 10-day running mean of 30min rainfall accumulation is below 0.05 mm

for 14 consecutive days (e. g. Fig. 6). For both SOS and EOS, the rainfall criterion itself is enough in sub-tropical and Mediterranean-like climates. Measurements from the flux tower at Skukuza site are used to locate the SOS and EOS for 6-year period. Results are shown in Fig. 6 with SOS and EOS marked as green and yellow triangles, respectively.

Start and end of greening season defined by the Ati et al. (2002) criteria in Fig. 6 are overlaid by time-series of seven different variables including both observed (temperature, LAI, FPAR, rainfall, 16 cm soil moisture) and diagnostic ones (Bowen ratio, plant available water fraction). For easier comparison purposes periods between SOS and EOS are shaded, denoting “greening” (or “wet”) seasons. Due to missing records of temperature at flux tower, a detection of SOS for the year of 2003 is missing. Leaf Area Index and FPAR independently observed by MODIS are presented as a reference only. Detected SOSs correspond not only to the rainfall events but to the soil moisture as well. *Plant available water fraction* integrates rainfall accumulation, meaning that it can serve as good criterion for detection of SOS. On the other hand, a detection of EOS shows equally good results with somewhere more disagreement to the MODIS LAI.

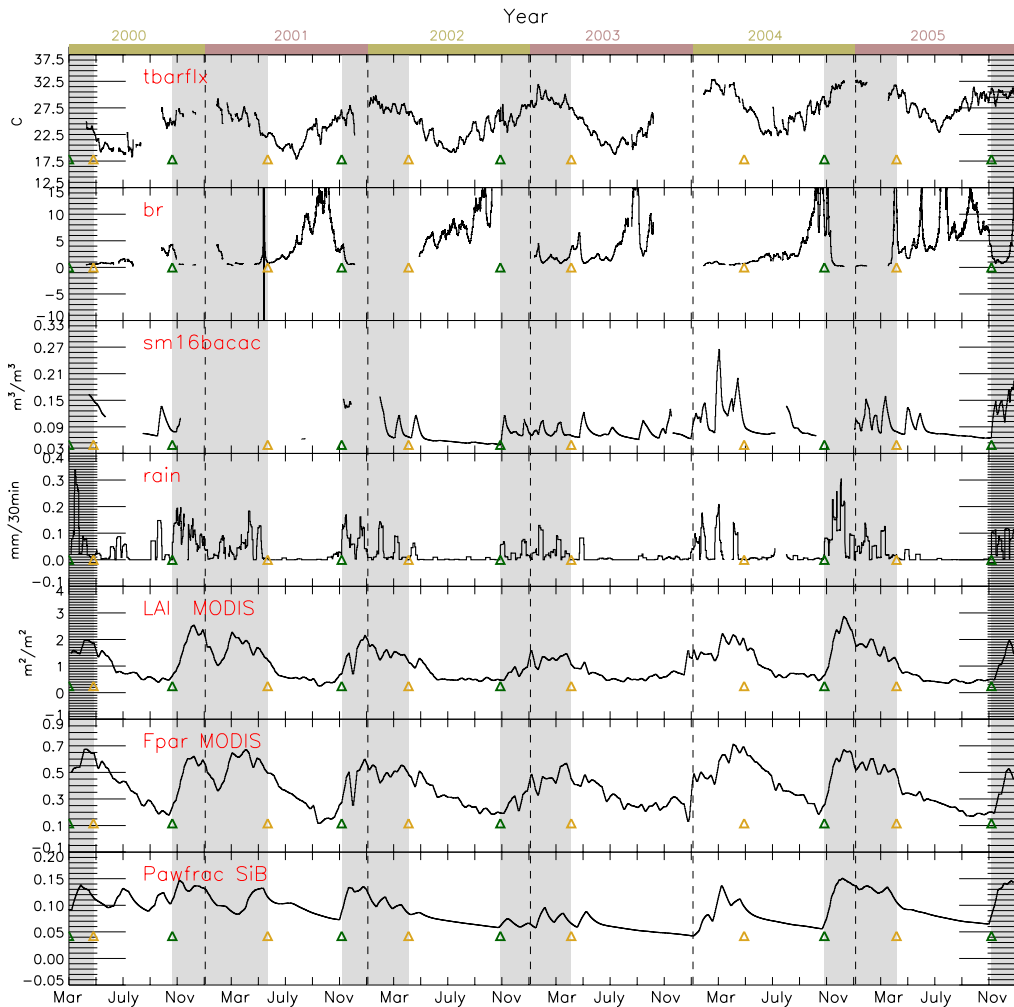


Figure 6 Comparison between different 10-day running mean forecasted and observed parameters and their relation to detected start (SOS) and end (EOS) of greening season; green triangles – SOS; yellow triangles – EOS; each of detected greening seasons is shaded; tbarflx- temperature; br- Bowen ratio; sm16bacac – soil moisture at 16cm depth; rain – rainfall accumulation; zlt MODIS – leaf area index detected by MODIS; Fpar MODIS – Fpar detected by MODIS; pawfrac SiB - plant available water fraction diagnosed by SiB

It is worth mentioning that climatology of Skukza site (Chapter 2) suggests that vegetation (and therefore greening season as well) is rain-driven, meaning that temperature condition in SOS detection shouldn't play a role. As a matter of fact, if carefully examined, Fig 6 supports this objection, meaning that the SOS in 2003 could be located just by looking at rain condition. And, indeed it could be. Temperature condition suggested by Ati et al. (2002) is unnecessary at climates such as Skukuza'a.

4.2 Prediction of greening season

The results presented in this section refer to Skukuza site located in Kruger Park, South Africa (in Figure 4 labeled as S0). Table 2 lists all vegetation types present at Skukuza site together with percentage of the area covered by each, as represented in SiB3 (see Appendix B for distribution of all sites vegetation). A time step of 600s is used to run the model. Two runs are performed. The first using the original *vpd-method*, and the second using new, *pawfrac-method*, both as described in Chapter 3.

Table 3 Distribution of phenological functional types present at S0 - Skukuza site.

Phenological functional types	Area of coverage (%)
Grass C4	58.7
Grass C3 Non-Arctic	9.2
Deciduous Broadleaf Trees (tropical)	12.3
Deciduous Broadleaf Shrubs (temperate)	12.7
Bare Ground	7.1

4.2.1 GSI and its contributing factors

Figure 7 shows timeseries of GSI and its governing factors at Skukuza site for the time period from January 1st 2000 to December 31st 2005 as forecasted by SiB3. The first two months of the period should be ignored since valid meteorology drivers are not available prior March 1st 2000. Upper plot is a result of the first run, the one using Eq. (1)-(8) where water vapor pressure deficit, as diagnosed from the observed tower data, is used to calculate the moist factor as in Eq. (2). Or in other words, the upper plot presents air-moisture-based seasonal growth factors. The lower plot shows a result of new technique,

the one based on soil moisture (i.e. *pawfrac*). Shaded areas are wet seasons as presented in Fig. 6. In both plots, the GSI is given by black solid line, while its governing factors: temperature, light and moisture, are plotted as colored dashed lines in: red, blue and green, respectively.

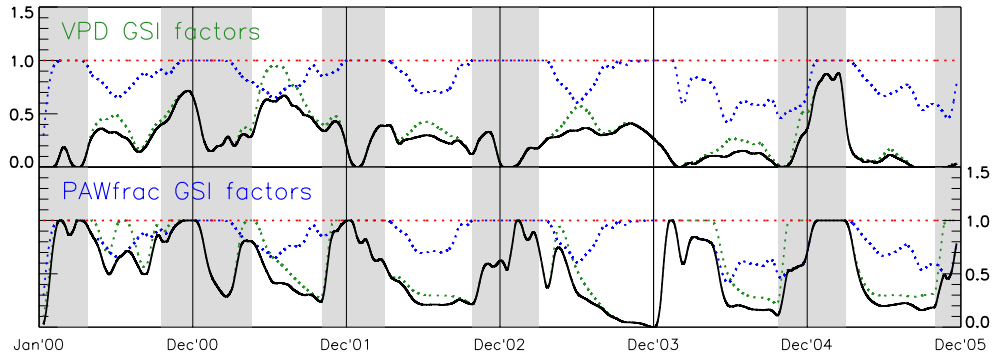


Figure 7 Growing Season Index –GSI (in black) and its contributors: temperature, light and moisture factors (in red, blue and green, respectively) at Skukuza site for time period from January 1st 2000 to December 31st 2005, given by SiB3 using *vpd*-method (upper plot) and *pawfrac*-method (lower plot). All values are 10-day running means.

According to Eq. (1) and the curves in Fig. 7, the moist factor (green line) can be considered as a main governing factor of the GSI value. Based on the climate characteristics of Skukuza site (description in Chapter 2) the model correctly simulates temperature and light factors that appear to always be favorable for plant production having their values above 0.5 at all times. Therefore, the moist factor is what essentially limits the GSI. This is a good representation of how we believe the nature functions. However, when focused on the moist factor only, some intriguing differences between the two methods appear. When water vapor pressure deficit is used to define the moist factor, the seasonality of the GSI is not obvious. Using the shaded areas to get an approximate location of the start and duration of wet seasons, some inconsistencies are obvious. First, the GSI curve (upper plot) sometimes appears to be lower during wet seasons than the dry ones (e.g. Dec '02 vs. June '03). The second, there are significantly long intervals of GSI value being at zero that are

placed in the middle of what is expected to be a wet season (e.g. Jan to Feb of '00 and '01, Feb to April '04). The latter suggests unfavorable conditions for plant growth during periods when the growth is expected to be the strongest, while the prior implies that plants can grow in months that are known to be characteristic by completely brownness of vegetation.

On the other side *pawfrac-method* GSI curve in the lower plot behaves close to what one would expect, with clear oscillation in its amplitude, alternating between periods when close to value of 1 and those when close to zero. At same time these intervals are in good temporal agreement with what is detected to be alternation of wet and dry seasons. When compared to the *vpd-method* the new method has greater maxima that are almost always equal or close to the value of 1, which will certainly lead to greater production of plants with more green mass. Another, maybe not so obvious, feature is that an initial increase in GSI value is steeper in the *pawfrac-* than in *vpd- method*. This is more likely to be closer to the nature of the greening in the rain-driven grasslands where long periods of brownness are replaced by green within a couple of weeks.

Sudden, occasional drops in the GSI value within wet seasons are present in both plots but more meaningful in the *pawfrac-method*. For example, in the lower plot of Fig. 7, GSI drops significantly during the first trimester of '01. As it will be shown later, these drops are closely related to the extended periods of precipitation absence, which resulted in drying the soil and decrease in soil moisture given by SiB. However, in the *vpd-method* (e.g. January '02 and '03, as well as end of '03) the drops are not related to the absence of plant available moisture, as the moist factor supposes to suggest, but rather to just the fact that air during these periods was relatively dry.

Overall, when the two methods GSIs are compared, even without looking at what they result in (in terms of LAI) the conclusion is that *pawfrac-method* is more realistic.

4.2.2 Leaf Area Index – LAI

The forecasted 6-year time period at Skukuza site captures most of the six growing seasons during that time. In Fig. 8 LAI as calculated by SiB3 using both methods (*vpd* in green, and *pawfrac* in blue) is plotted along with precipitation measured at the site (red line in top plot). This side-by-side comparison allows an easy appraisal of how each of the methods performs.

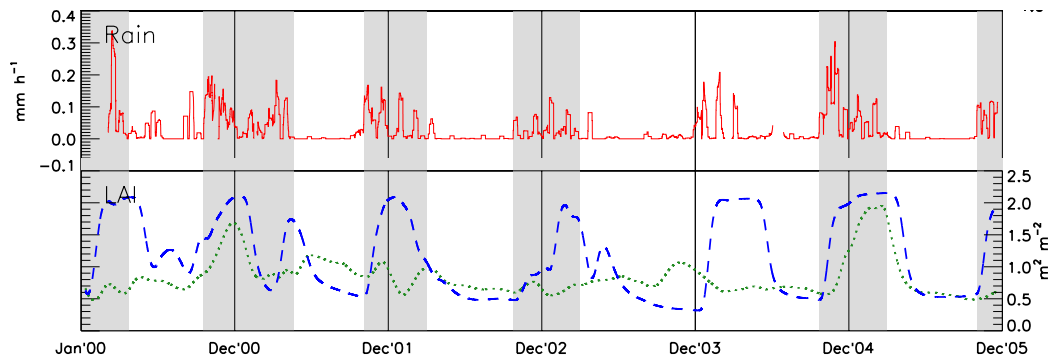


Figure 8 Rain (top, red) and LAI (at bottom with y-axes on the right) at Skukuza site for time period from January 1st 2000 to December 31st 2005. Vpd-method LAI is given by green dotted line while *pawfrac*-method is given by blue dashed line. All values are 10-day running means. Shaded areas denote greening seasons as detected by criteria defined in Chapter 3.

With six greening seasons given, one would expect to see about six pronounced peaks of LAI. *Pawfrac-method* predicts this kind of greening cycle, while *vpd-method* results in, to some extend, chaotic oscillation of LAI that is hard to relate to either precipitation events or wet seasons. The greening of the two methods agrees only in two seasons (markers at Dec '00 and Dec '04). Another clear difference is in the amplitude. Although overall the methods tend to have similar LAI minima, *pawfrac-method* absolute minimum appears more realistic with the value of about 0.3. On the other side *pawfrac-method* produces

significantly higher maxima exceeding LAI of 2.0 in every single season at same time having pronounced periods of greening and drying that are closely related to the precipitation and therefore wet seasons. *Vpd-method* LAI also reaches very similar maxima values but only in two seasons (Dec '00 and Dec '04) implying that this maximum is not an artifact of *pawfrac-method* but rather a realistic estimate of green mass being developed at the site. However, at other times *vpd-method* LAI values are hard, if possible at all, to justify. The curve simply oscillates often producing unrealistic drops and peaks at times that do not correspond to oscillations recorded, or at least expected, at the site with such a pronounced seasonality of greening, as Skukuza site is.

Somewhere surprising behavior of *pawfrac-method* LAI curve can be noticed as well. In the wet seasons of '00/'01 LAI experiences “unexpected” drop. However, this local minimum is a result of LAI decrease triggered by unusually long period (about two weeks) of no rain during this wet season. Therefore, this is quite possible to appear in the nature and, as we will see in evaluation section that follows, documented as well. As a matter of fact, the decrease of LAI in January to March of '01 is present in *vpd-method* as well indicating that even atmospheric moisture during that period was low.

4.3 Evaluation

Due to the deficiency of LAI measurements at Skukuza site, we evaluate the results presented in section 4.2 through the comparison of the observed and forecasted fluxes of carbon, and latent and sensible heat at the site location, and through the estimation of the *new-method* results at a number of different sites located in different climates where some do have observations of LAI. Although not ideal, this is the best available method for

verifying results of this study. Amount of leaves directly influences latent and sensible heat through evapotranspiration as well as carbon flux through photosynthesis process. On the other side, using different climates and biomes to test the method provides an evaluation of the robustness of the new technique. All results and comparisons in this section are given through 10-day running means, while corresponding plots of monthly means are provided in Appendix A. Observations are plotted when valid data are available, requiring at least 30% of valid data within the each of 10-day averaging intervals. These together provide an evaluation of the methodology, results and potential for global application of this method that is attempting to capture greening season onset at rain-driven biomes.

S0 - Skukuza, Kruger Park, South Africa

To start with, we compare the fluxes of carbon, and latent (LH) and sensible heat (SH) at site S0. In Fig. 9 observed (red line) and forecasted values (*vpd-method* in green, *pawfrac-method* in blue) of these fluxes are plotted along with LAI (the one already seen in Fig. 8). At glance, one can note that the two methods follow each other during entire period of integration pretty closely. Therefore it can be argued that the new-method simply produces fluxes that respond to the changes in LAI and meteorology in the manner that is expected without introducing any new, potentially unrealistic, behavior when compared to the old one.

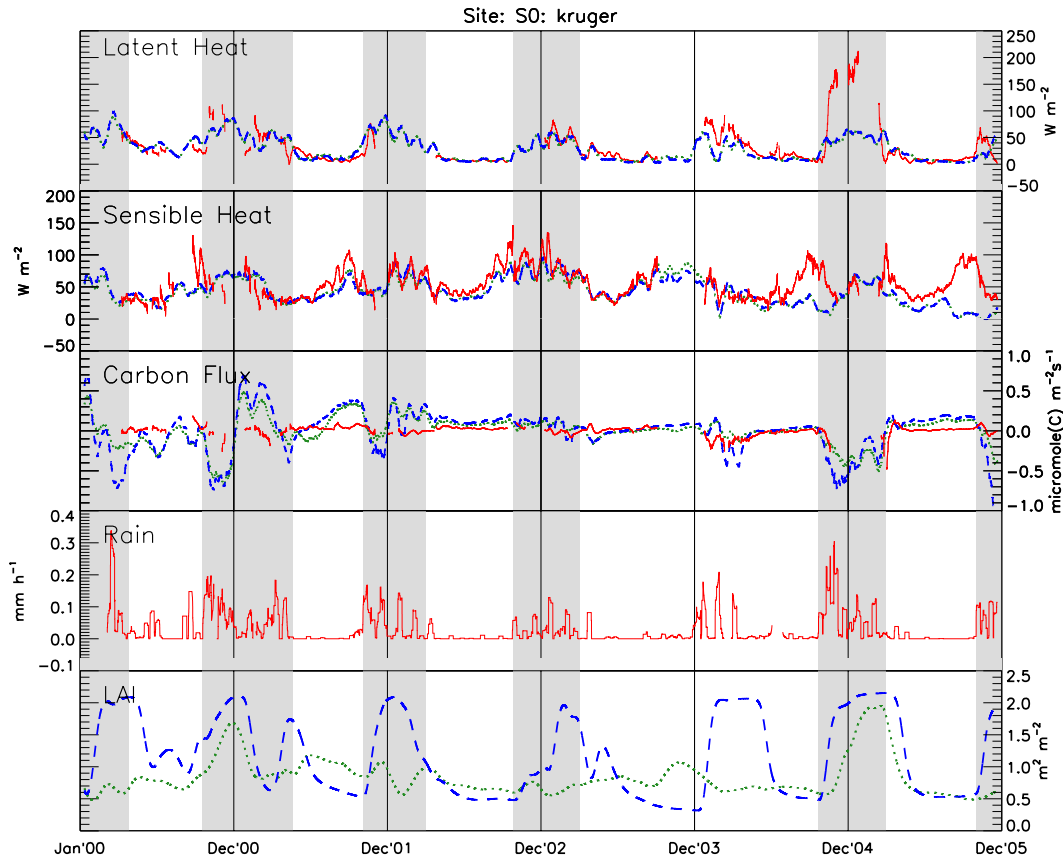


Figure 9 Comparison of the observed (red) and forecasted fluxes (from the top: Latent Heat, Sensible Heat and Carbon) produced by *vpd-method* (green) and *pawfrac-method* (blue), precipitation (second from the bottom), and LAI (the bottom plot) [observed (crosses) and forecasted (*vpd-mehtod* in green, *pawfrac-method* in blue)] for site S0 - Skukuza, Kruger Park, South Africa for period January 1st 2000 till December 31st 2005.

Latent heat flux of both methods increases during wet seasons being, in general, in very good agreement with observations. Sensible heat flux has more pronounced difference between the two methods, with *new-method* being closer to the observed curve. Although the difference between the two is small, it represents an improvement that may play an important role when processes at smaller than seasonal time scales are considered. When looking at the carbon flux, *vpd-method* performs better. However, both curves have difficulties to closely follow observations indicating possible problems with either the observations or the physics that models use to diagnose the carbon flux and its contributors.

The fact that new-method performs slightly better or worse than the old one, however, is not as important finding as the that the fluxes of the two methods follow each other closely during the entire integration interval, meaning that both methods are very similar overall and changes made by *pawfrac-method* are not changing the balance SiB had previously established using *vpd-method*.

In terms of LAI, a *pawfrac-method* curve reflects more of wet/dry season related oscillation than *vpd-method*. At same time *pawfrac-method* LAI amplitude reflects better the values found in the literature for the period presented here. Williams et al. (2009) report an overall LAI average of about $1.1 \text{ m}^2 \text{ m}^{-2}$ for 2000-2004 period with LAI maxima during wet seasons as high as $2.0 \text{ m}^2 \text{ m}^{-2}$. At same time decreases of LAI value seen during wet season can be related to the presence of non-C4 grass vegetation at the site, whose greening is not tied to the onset of wet season. Trees and grasses in savanna systems have different seasonal leaf area dynamics, controlled by different environmental cues producing dips in LAI time-curve as those seen in Fig. 6. This is addressed in Archibald and Scholes (2007).

Therefore, a conclusion is that by using an integrated soil moisture information the new-method in the phenology model is capable to realistically represent both: 1) LAI, and 2) seasonal cycle related to alternation of wet and dry seasons.

S1 - Lethbridge, Canada

Although the new-method is developed with the goal of bringing an improvement to the seasonal cycle of LAI at places where vegetation is strongly driven by precipitation, we test the method's performance at a whole variety of climates as well, with the goal to show how plant growth dependence on soil moisture can pre successfully modeled. At site S1

vegetation is driven with all three factors (temperature, light and moisture). Figure 10 shows the GSI and contributing factors, given by the two methods, at the place where even *vpd*- and *pawfrac*- moisture factors are significantly different, the fact that temperature is what really drives the vegetation results in basically same GSI curves with the difference that *pawfrac-method* has higher amplitude.

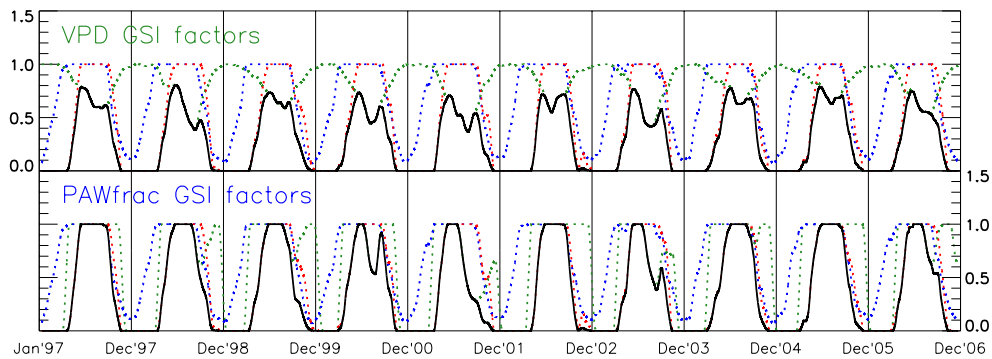


Figure 10 Growing Season Index -GSI (in black) and its contributors: temperature, light and moisture factors (in red, blue and green, respectively) at Lethbridge, Canada for time period from January 1st 1997 to December 31st 2006, given by SiB3 using *vpd*-method (upper plot) and *pawfrac*-method (lower plot). All values are 10-day running means.

This higher amplitude of GSI naturally results in higher LAI values, which is clearly shown in Fig. 11. Here, similarly as in corresponding figure of S0, all fluxes are very close to each other when the two methods are compared. Appendix A provides monthly means of all variables shown in Fig. 11 plus meteorological drivers used by SiB where it can be seen that the sub-freezing temperatures are the reason of green-plant absence during winter time. On the other side, some, occasional LAI observations are available at this location (black crosses in the lower panel of Fig. 11). They show very strong agreement to the SiB values in terms of seasonal cycle. However, the amplitude of the *vpd*-method LAI is much closer (almost identical) to the observations of LAI.

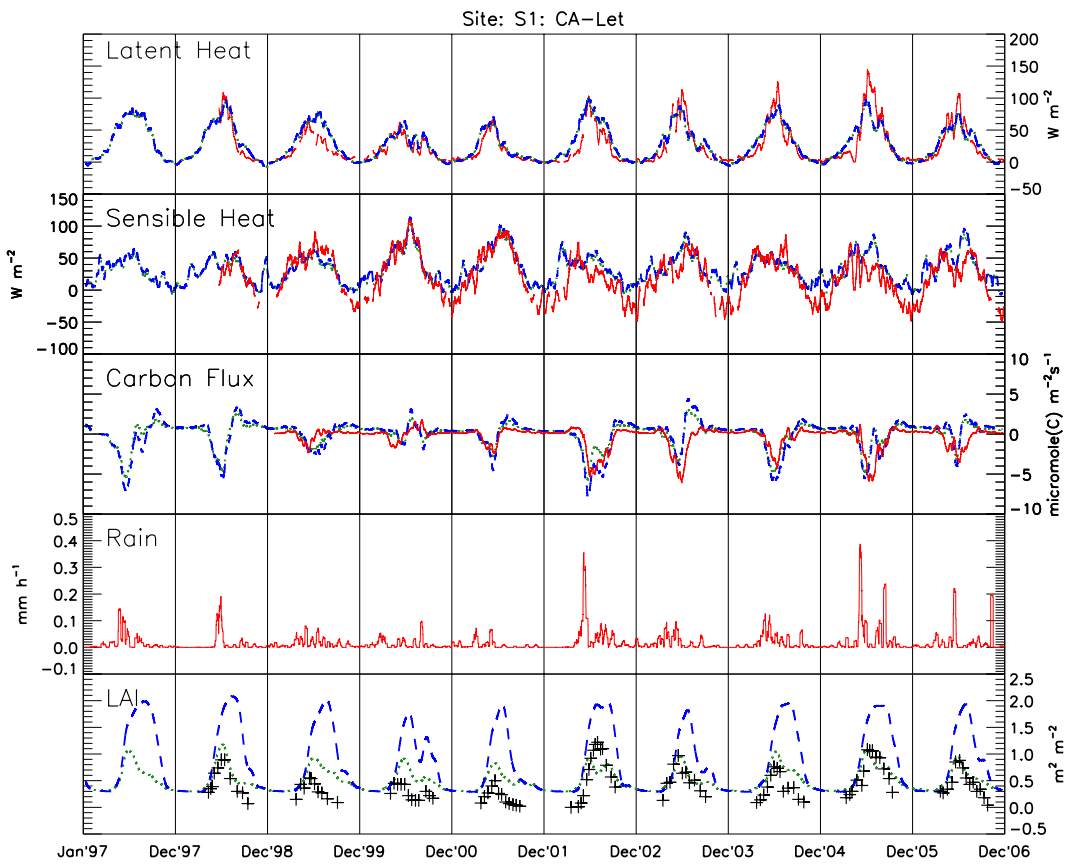


Figure 11 Comparison of the observed (red) and forecasted fluxes (from the top: Latent Heat, Sensible Heat and Carbon) produced by *vpd-method* (green) and *pawfrac-method* (blue), precipitation (second from the bottom), and LAI (the bottom plot) [observed (crosses) and forecasted (*vpd-mehtod* in green, *pawfrac-method* in blue)] for site S1 - Lethbridge, Canada for period January 1st 1997 till December 31st 2006.

The first conclusion could be that at the S1 site (a non-rain-driven vegetation site) the new-method succeeds in capturing the seasonal cycle of LAI but not in estimating its amplitude. However, as presented in Chapter 3, SiB parameters that define phenology state can influence the amplitude of LAI significantly and future work on adjusting those to be spatially dependent may easily remove those differences. For demonstration purposes only, we have altered a single parameter - Fparmax (or the maximum allowed Fpar value), for two most dominant vegetation types (see Appendix B) at this site by reducing its value by about 60%. The result is shown in Fig. 11a (note the difference in y-axis range of LAI panel in Figs. 11 and 11a). This simple adjustment has not only improved LAI estimate but

fluxes as well where now *pawfrac-method* performs better than *vpd-method*. Therefore, the conclusion is that *pawfrac-method* is capable of representing the nature of the plant growth (both, LAI and greening cycle) even at the sites that experience strong oscillations of all three GSI contributors.

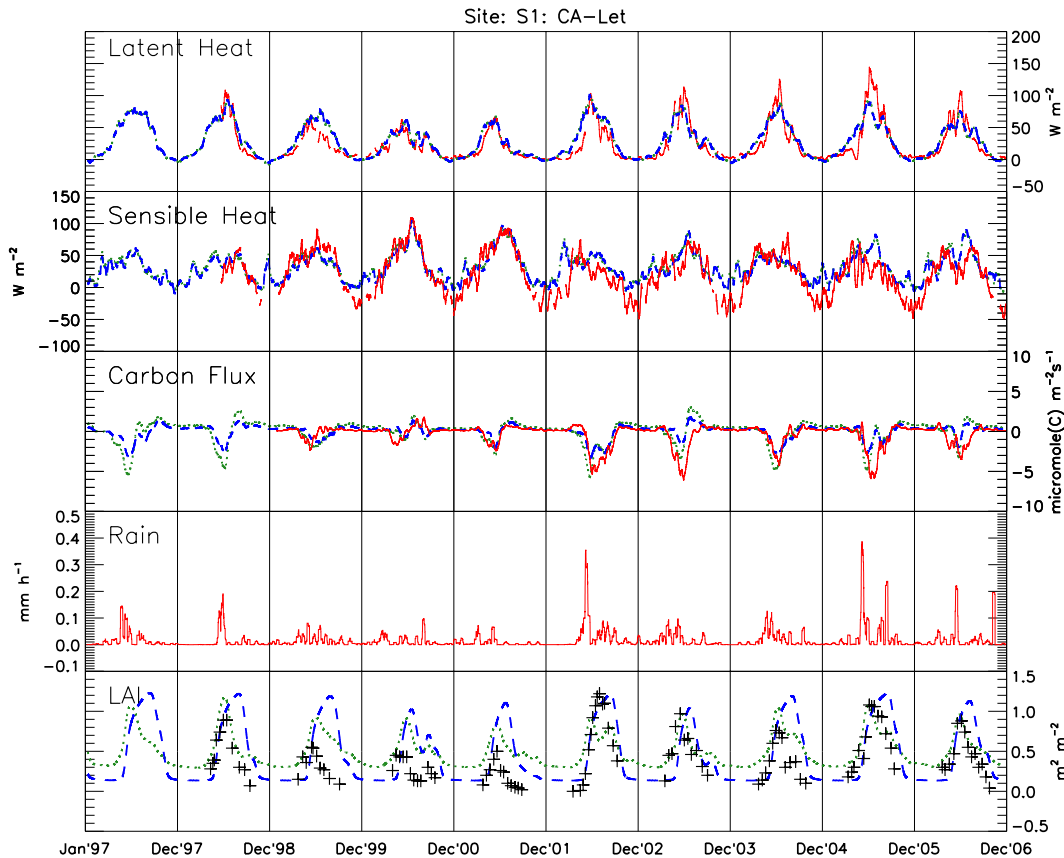


Figure 11a Comparison of the observed (red) and forecasted fluxes (from the top: Latent Heat, Sensible Heat and Carbon) produced by *vpd-method* (green) and **adjusted pawfrac-method** (blue), precipitation (second from the bottom), and LAI (the bottom plot) [observed (crosses) and forecasted (*vpd-mehtod* in green, *pawfrac-method* in blue)] for site S1 - Lethbridge, Canada for period January 1st 1997 till December 31st 2006.

Adjusting the parameters and defining their spatio-temporal dependence is beyond the scope of this study and is left for the future work. This process will require an employment of MODIS or similar observations that can provide good temporal and spatial information to full data assimilation package that will be integrated into phenology model.

S2 - Shidler Tallgrass Prairie, Oklahoma, US

Another example of the site where GSI value of the two methods does not differ a lot is S2, a site where constantly sufficient amount of precipitation provide very similar signatures of both air and soil moisture, leaving the GSI to be driven mainly by temperature and radiation (light). Figure 12 shows time-series of GSI and its contributors, where the only difference between the two methods is the amplitude of GSI, with distinction of having larger minima than S1 site due to the fact that temperature rarely approaches freezing level (see monthly means for S2 in Appendix A).

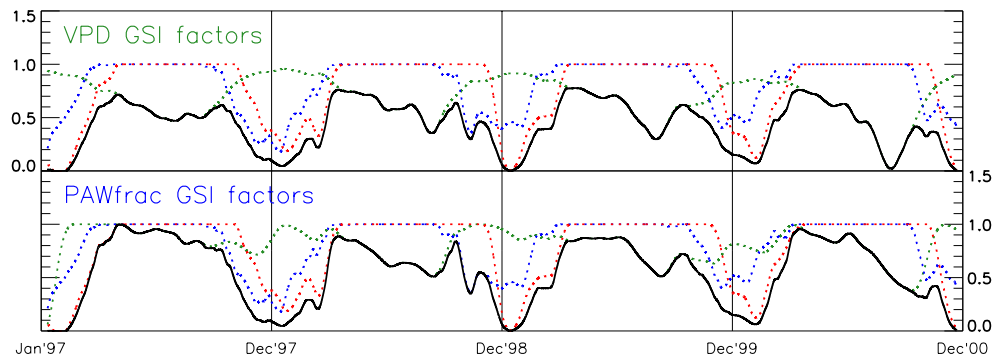


Figure 12 Growing Season Index -GSI (in black) and its contributors: temperature, light and moisture factors (in red, blue and green, respectively) at Shidler Tallgrass Prairie, Oklahoma, US for time period from January 1st 1997 to December 31st 2000, given by SiB3 using *vpd-method* (upper plot) and *pawfrac-method* (lower plot). All values are 10-day running means.

From Fig. 12 and S2 climate description (Chapter 2) we can expect to see very similar LAI result as for S1, although the reason this time is different, instead of having the dominance of the temperature as governing factor for GSI as at S1 site, the combination of both temperature and radiation being low forces the season to end. However, GSI never reaches the zero, implying that LAI should stay fairly high during a year.

Figure 13 shows the same comparison of the fluxes and LAI as earlier where precipitation provides an insight of the moisture availability (specific humidity values available on monthly means plot in Appendix A). Observed LAI is added plotted (black

crosses) in the last plot. As expected the result is very similar to that of S1 site with *pawfrac-method* fluxes being slightly closer to observations and LAI having the same seasonal cycle with higher amplitude when the *new-method* is used. The only difference here is that the *new-method's* LAI amplitude is closer to the observed values of LAI for the most of the period. Observed LAI values exceed the prognosed ones during green seasons and clearly reach zero in winter months, which both methods fail to recognize (although there was a fire event in March of '00). Again, using the same arguments as in S1 site case, we conclude that although phenology model (as it is) is incapable of reproducing the exact amount of the green plant area at this type of biome-climate combination, the *new-method* does very well in reproducing the seasonality of LAI, at same time keeping the fluxes at least equally good as the original *vpd-method* and slightly better LAI (according to available measurements).

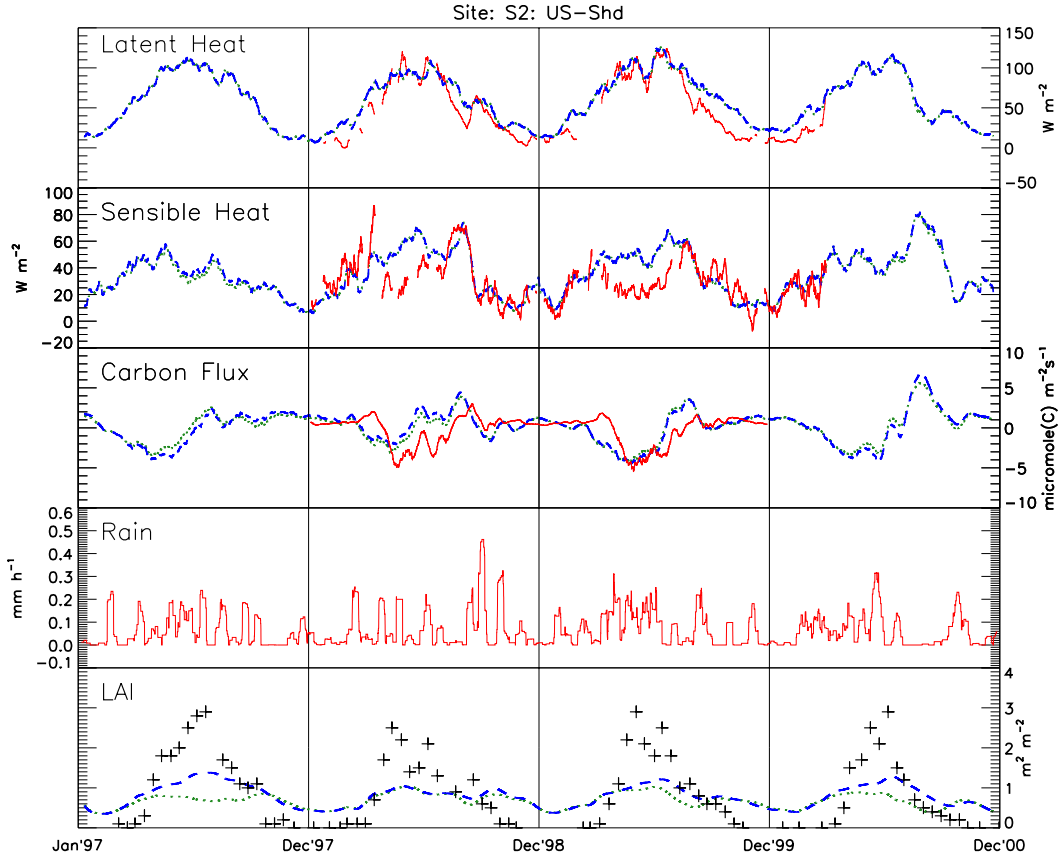


Figure 13 Comparison of the observed (red) and forecasted fluxes (from the top: Latent Heat, Sensible Heat and Carbon) produced by *vpd-method* (green) and *pawfrac-method* (blue), precipitation (second from the bottom), and LAI [(the bottom plot) - observed (crosses) and forecasted (*vpd-mehtod* in green, *pawfrac-method* in blue)] for site S2 - Shidler Tallgrass Prairie, Oklahoma, US for period between January 1st 1997 till December 31st 2000

S3 - Fermi Prairie, Illinois, US

Based on its climate characteristics, Fermi Prairie site can be classified somewhere in between sites S1 and S2 with sufficient amount of moisture provided by equally spread precipitation yearlong (see Fig. 15 – Rain, and Fig. 14 – Moisture Factor) and temperature and radiation having pronounced seasonal cycles with somewhat longer warm seasons than at S1 site but significantly colder winters than at S2 site. Before the results are interpreted it is important to note that the soil appears unrealistically dry at the beginning of the second year due to the missing observations (missing observations of precipitation are replaced by zero). This results in *pawfrac-method* GSI curve being somewhat lower

than it would be with valid measurements. However, the two curves behave similarly. They follow each other by shape with *pawfrac-method* having slightly greater amplitude. This difference is not large and LAI values appear to be almost identical during the most of the integration interval (see Fig. 15). The exception is of course the mentioned period of no precipitation observations.

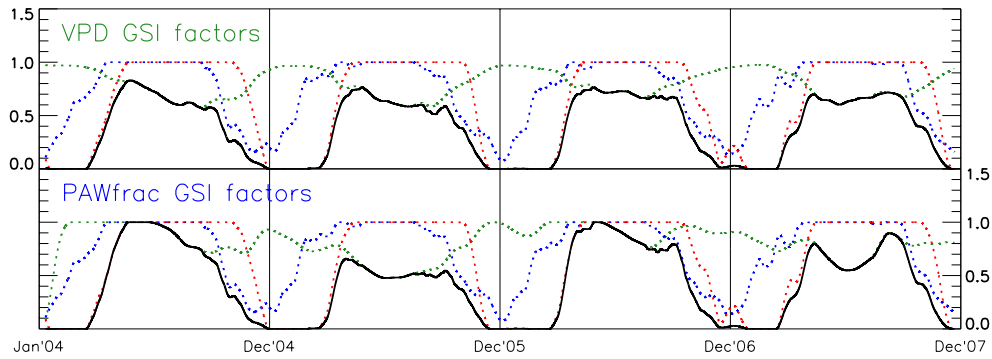


Figure 14 Growing Season Index -GSI (in black) and its contributors: temperature, light and moisture factors (in red, blue and green, respectively) at Fermi Prairie, Illinois, US for time period from January 1st 2004 to December 31st 2007, given by SiB3 using *vpd-method* (upper plot) and *pawfrac-method* (lower plot). All values are 10-day running means.

However, when compared to observations of LAI both methods underestimate the amplitude. This is clearly visible in coincide overestimate of sensible and underestimate of latent heat (Fig. 15). The reason for this, as illustrated at S1 site, lays in the usage of fixed, temporally and spatially independent, phehenology parameters.

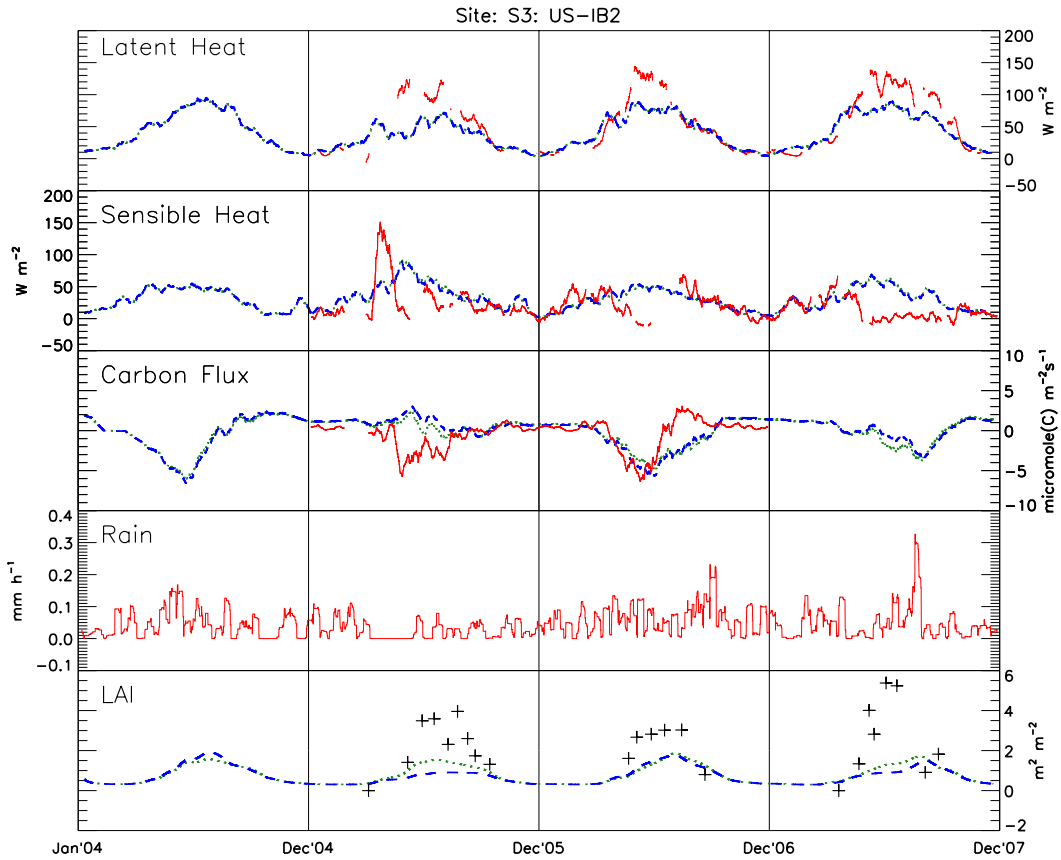


Figure 15 Comparison of the observed (red) and forecasted fluxes (from the top: Latent Heat, Sensible Heat and Carbon) produced by *vpd-method* (green) and *pawfrac-method* (blue), precipitation (second from the bottom), and LAI [(the bottom plot) - observed (crosses) and forecasted (*vpd-mehtod* in green, *pawfrac-method* in blue)] for site S3 - Fermi Prairie, Illinois, US for period between January 1st 2004 till December 31st 2007

Overall, the conclusion can be that both methods perform equally well in this environment and that the new-method does not show any drawbacks compared to the old one.

S4 - Vaira Ranch, California, US

Vegetation at Vaira Ranch is, to some extent, rain-driven but not as exclusively as at S0 site. Greening is strongly linked to the wet season, but the opposite phase of the temperature and light factors play an important role in defining GSI value. In Fig. 16 light and temperature factors are at maxima during dry part of the year but drop significantly in wet season. This delays the SOS relative to start of the rain season, resulting in not as steep

LAI increases (Fig. 17) as at S0 site. The two GSI curves in Fig. 16 differ in amplitude when compared against each other. Also *pawfrac-method* GSI does not experience a minimum in the second part of the greening season..

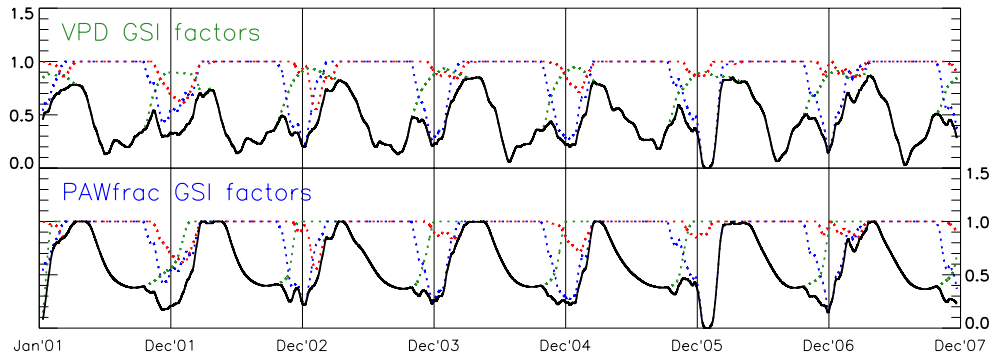


Figure 16 Growing Season Index -GSI (in black) and its contributors: temperature, light and moisture factors (in red, blue and green, respectively) at *Vaira Ranch, California, US* for time period from January 1st 2001 to December 31st 2007, given by SiB3 using *vpd-method* (upper plot) and *pawfrac-method* (lower plot). All values are 10-day running means.

The differences between observed and the two prognosed LAI curves in Fig. 17 are well reflected through fluxes comparisons. *Pawfrac-method* seems to perform better in terms of LAI at the SOS, but *vpd-method* is better afterwards, although both methods fail to follow observations in the second part of the growing season. This behavior is, however, questionable. The fact that observed LAI reaches zero value indicates either the presence of fire events, or that the vegetation considered in measurements of LAI at the site is grass exclusively and therefore gets dried out in summer. SiB on the other side (see Appendix B) has approximately 25% of vegetation at this site defined as Evergreen Broadleaf Shrubs. This is the reason of having modeled LAI minima not lower than $0.5 \text{ m}^2 \text{ m}^{-2}$ at any time.

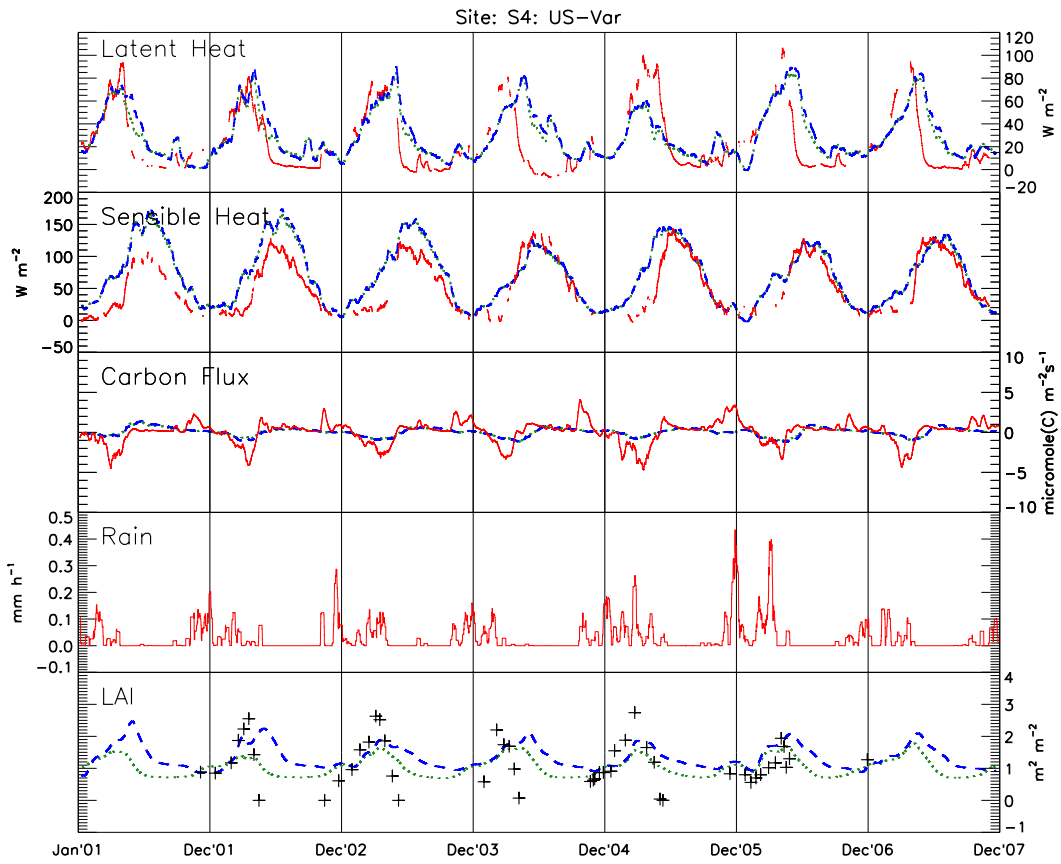


Figure 17 Comparison of the observed (red) and forecasted fluxes (from the top: Latent Heat, Sensible Heat and Carbon) produced by *vpd-method* (green) and *pawfrac-method* (blue), precipitation (second from the bottom), and LAI [(the bottom plot) - observed (crosses) and forecasted (*vpd-mehtod* in green, *pawfrac-method* in blue)] for site S4 - Vaira Ranch, California, US for period between January 1st 2001 till December 31st 2007

Since he observations have no fire events on the record we assume that the difference between observed and modeled LAI originates in the model's definition of vegetation and conclude that *pawfrac-method* may perform fairly well for vegetation that are rain-driven but not as strongly as those at site where the method was developed (S0).

S5 - Fort Peck, Montana, US

Fort Peck grasslands are another example of the site where all three factors drive GSI. Being at 48°N the site experiences strong seasonal changes in temperature and radiation,

while the discrepancies between soil and air moisture (Fig. 18) result in different amplitude and shape of the two methods GSI curves.

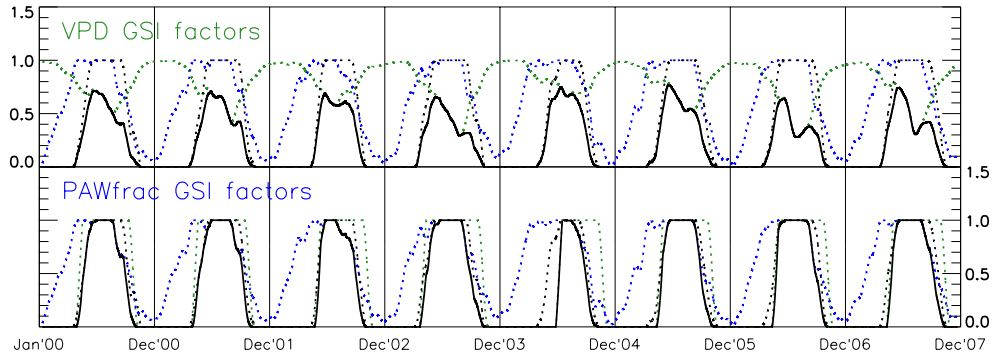


Figure 18 Growing Season Index -GSI (in black) and its contributors: temperature, light and moisture factors (in dotted black, blue and green, respectively) at *Fort Pack, Montana, US* for time period from January 1st 2000 to December 31st 2007, given by SiB3 using *vpd-method* (upper plot) and *pawfrac-method* (lower plot). All values are 10-day running means.

Unfortunately no observations are available for this site (Fig. 19 uses model drivers data to show precipitation). However, we still believe that Fort Pack serves as a valid evaluation of the *pawfrac-method* since site documentation (CPPA- Climate Prediction Program for the Americas) states that LAI values have pronounced seasonality with its maxima ranging from 1 to 2 m² m⁻². According to these records, *pawfrac-method* performs better than *vpd-method* when it gets to the LAI amplitude prediction (Fig. 19). Seasonality is captured equally well by both methods, while *pawfrac-method* tends to produce more realistic shape of the curve with no local minima during the greening seasons as in *vpd-method* case. The difference in the amount of green mass that methods produce is clearly reflected through fluxes as well.

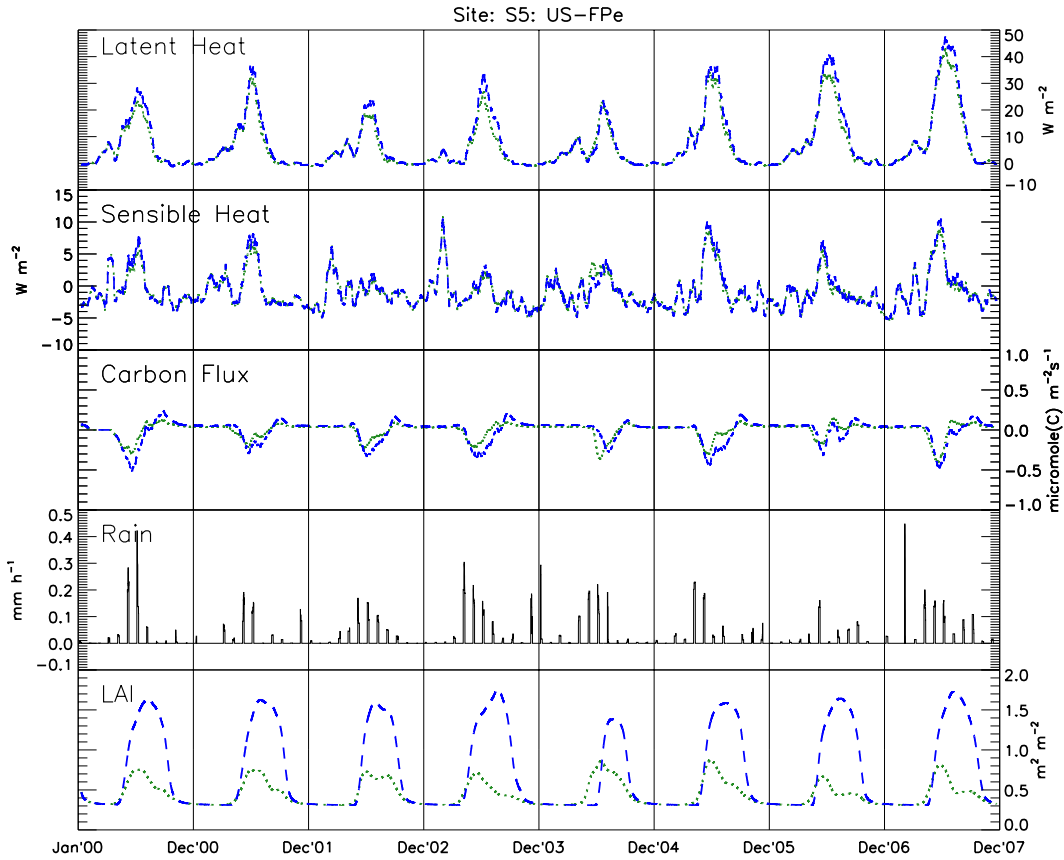


Figure 19 Comparison of the forecasted fluxes (from the top: Latent Heat, Sensible Heat and Carbon) produced by *vpd-method* (green) and *pawfrac-method* (blue), precipitation from driver's data (second from the bottom), and forecasted LAI (the bottom plot, *vpd-mehtod* in green, *pawfrac-method* in blue) for site S5 - Fort Peck, Montana, US for period January 1st 2000 till December 31st 2007.

S6 - Fazenda Nossa Senhora, Brazil

This site is in deep tropics, in an area dominated by grasslands developed as a consequence of Amazon deforestation. Therefore, all conditions for plant growth are expected to be ideal and reflected through the high values of GSI governing factors at all times. Precipitation in this region provides sufficient soil moisture for plant development a year around. The site, however, experiences a short dry season (2-3 months long) between August thorough November and this period should be the time when GSI may show some drops, if any.

In Fig. 20 both temperature and light factors are constantly at maximum value while GSI curves overlap with moisture factor curve, meaning that vegetation at the site is rain-driven. However this is quite different than rain-driven vegetation at S0 – Skukuza site, for two reasons. First, the soil moisture is relatively high even during the “dry season”, and second, instead of having a complete loss of leaves, plants rather just decrease the amount of green mass during the dryer intervals, which are also two to three times shorter than those at S0 site.

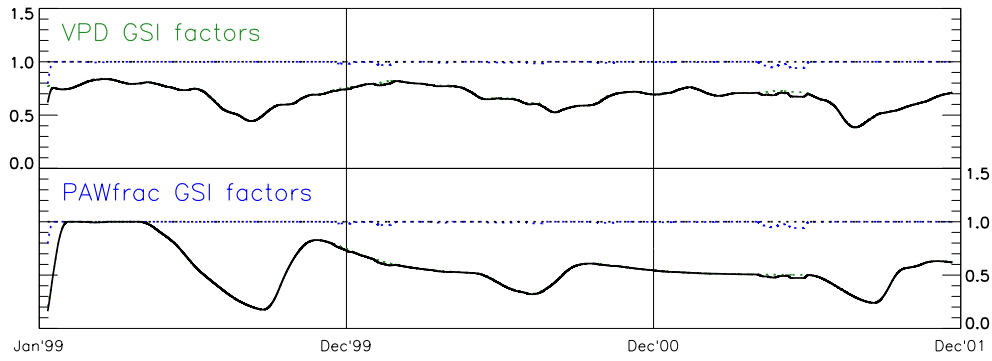


Figure 20 Growing Season Index –GSI (in black) and its contributors: temperature, light and moisture factors (in dotted black, blue and green, respectively) at Fazenda Nossa Senhora, Brazil for time period from January 1st 1999 to December 31st 2001, given by SiB3 using *vpd-method* (upper plot) and *pawfrac-method* (lower plot). All values are 10-day running means.

Large amount of missing data complicates the interpretation of such discrepancies between the modeled and observed SH and LH (Fig. 21). While modeled SH flux seems to follow the cycle of the observed one, LH flux appears to be more chaotic.

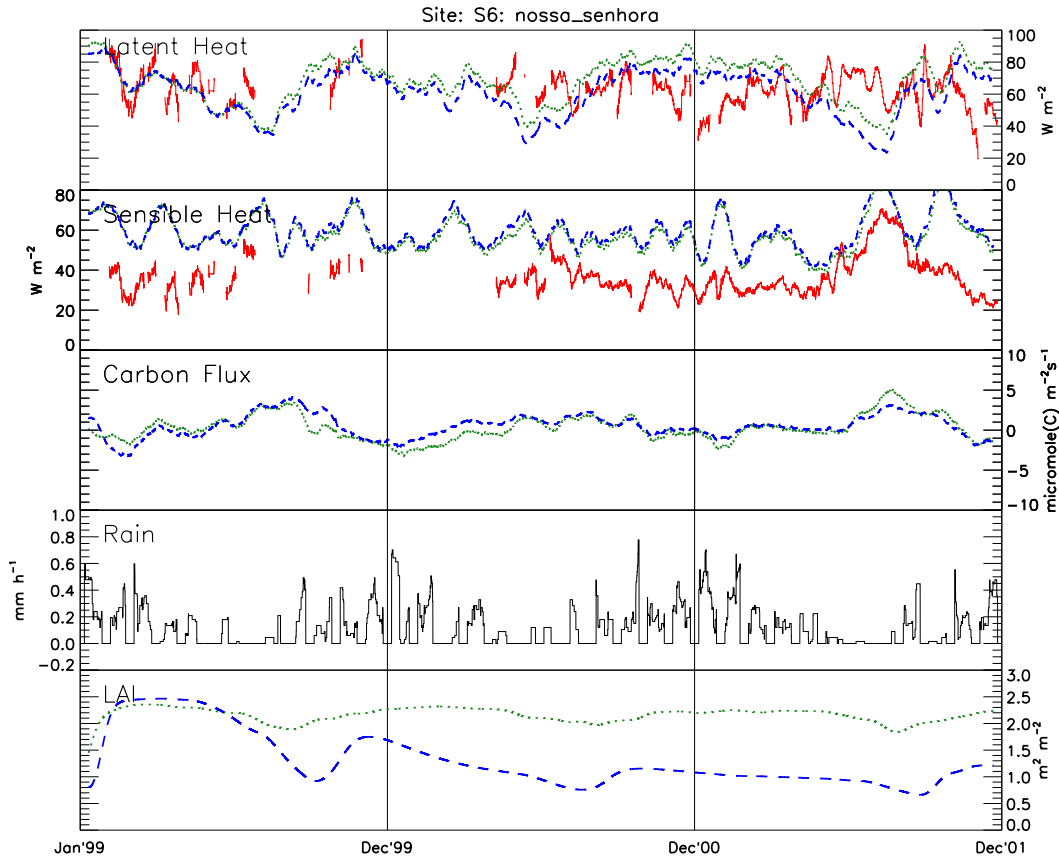


Figure 21 Comparison of the observed (red) and forecasted fluxes (from the top: Latent Heat, Sensible Heat and Carbon) produced by *vpd-method* (green) and *pawfrac-method* (blue), precipitation from driver's data (second from the bottom), and LAI [(the bottom plot) forecasted *vpd-method* in green, *pawfrac-method* in blue] for site S6 - Fazenda Nossa Senhora, Brazil for period January 1st 1999 till December 31st 2001.

On the other site observed LAI values speak in favor of SiB. Zanchi et al. (2009) provide measurements of LAI at the site for much longer period than the one simulated by SiB (Fig 22). Although measurements are done only twice a year, we can see that LAI cycle (given as IAF in Fig. 22) appears to be very similar to the one predicted by SiB (given in Fig. 21). While both methods perform similar in capturing the greening cycle, the *pawfrac-method* can be estimated as better performing when amplitudes are compared.

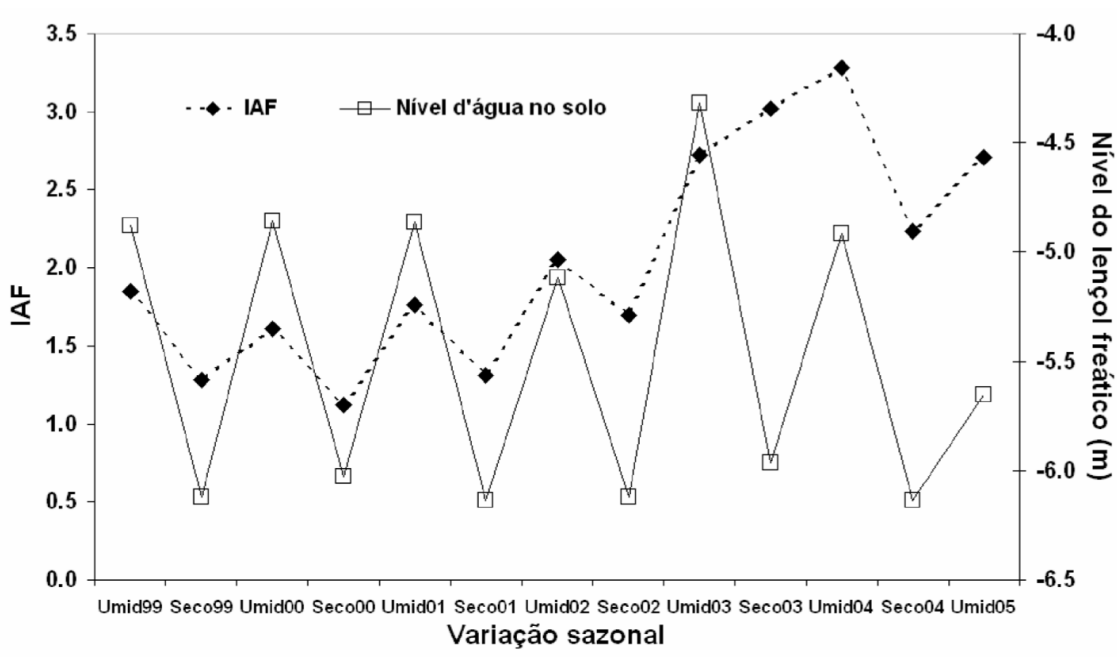


Figure 22 Observed LAI (dotted line with filled rhomboids) at S6 - Fazenda Nossa Senhora, Brazil for period January 1st 1999 till December 31st 2005. After Zanchi et al. (2009). IAF on y-axes stands for LAI. X-axes is time in 6 month increments labeled by year.

CHAPTER 5 Conclusions

A soil moisture-based method has been developed to improve phenology forecasts of LAI at rain-driven vegetation sites, such as grasslands and savannas. A potential available water fraction *pawfrac* has been used, as given by SiB, to imply soil conditions in the area of LAI prediction. The new proposed methodology modifies Jolly and Stöckli's definition of GSI, which now rather than using an air moisture deficit, bases its value on integrated soil moisture. This change has improved a seasonal response of predicted LAI related to the alternation of wet and dry seasons.

The method has been developed and tested on flux tower based observations of South Africa's savanna and then evaluated at other 6 grassland flux tower locations around the world with very distinct climatic variations. Before the results are compared to the observations of LAI (where available) a comprehensive comparison between the observed and modeled fluxes has been performed. After making sure the new method agreed to the original in their latent and sensible heat and carbon flux, the LAI time profile was compared with an existing model's results.

The new method has showed skill in capturing all three: start and duration of greening season, as well as amplitude of LAI during the season. The best results are obtained for C4 grass vegetation which is known as strongly rain-driven. The greatest improvement is seen at sites with pronounced, long dry season having the rain as only factor that drives vegetation growth. While improvements were still present, they were somewhat smaller at those sites where the oscillation in temperature and radiation is also important in defining plant growth conditions.

The goal of the study was to provide a potential for improvement in forecasting skills of greening season at places such as grasslands, where the currently used definition of GSI does not perform very well. This is done by employing information on soil moisture that is available to plant, which is more realistic representation of the nature than currently used air moisture-based method.

The results overall have shown that start and seasonality of the greening season have been correctly captured using the new method providing the best results in the areas of the greatest contrasts between dry and wet seasons. The proposed methodology is characterized by its moving averages introduced to allow easy temporal weighting adjustments that corresponds to the period and amplitude of dry to wet season oscillation. This allows for inclusion of data assimilation processes into the phenology model, which would provide spatial and vegetation type dependency to the temporal weights. This will bring the opportunity to expand the improvements seen here to the variety of climates seen at savannas sites and beyond.

It is certain that our ability to capture greening season of biomass still has to be improved and potentially be based on a more complex relations between the environment and plants than just the availability of water, heat and sunlight, but the introduction of soil moisture into this process is a good step foreword in our understanding of surface processes and carbon cycle.

References

Agriculture Canada (1987) The Canadian System of Soil Classification. Ottawa, Canada.

Andreae et al., 2002, Biogeochemical cycling of carbon, water, energy, trace gases, and aerosols in Amazonia: the LBA-EUSTACH experiments, *J. Geophys. Res.*, 107 (D20) (2002), p. 8066 <http://dx.doi.org/10.1029/2001JD000524>

Archibald, S. and Scholes, R.J. Leaf green-up in a semi-arid African savanna –separating tree and grass responses to environmental cues. *Journal of Vegetation Science* 18, 583 (2007).

Ati, O. F., Stigter, C. J., Oladipo, E. O. (2002), A comparison of methods to determine the onset of the growing season in northern Nigeria, *International Journal of Climatology*, vol. 22, Issue 6, pp.731-742.

Austin AT et al (2004) Water pulses and biogeochemical cycles in arid and semiarid ecosystems. *Oecologia* 141:221–235

Bach CS (2002) Phenological patterns in monsoon rainforests in the Northern Territory, Australia. *Australian Journal of Ecology*, 27, 477–489.

Baker, I.T., A.S. Denning, N. Hanan, L. Prihodko, P.-L. Vidale, K. Davis and P. Bakwin (2003), Simulated and observed fluxes of sensible and latent heat and CO₂ at the WLEF-TV Tower using SiB2.5. *Glob. Change Biol.*, 9, 1262-1277.

Baker, I.T., L. Prihodko, A.S. Denning, M. Goulden, S. Milller and H. da Rocha, 2008. Seasonal drought stress in the Amazon: Reconciling models and observations. *J. Geophys. Res.*, **113**, G00B01, doi:10.1029/2007JG000644.

Baldocchi D, Tang J, Xu LK (2006) How switches and lags in biophysical regulators affect spatial-temporal variation of soil respiration in an oak-grass savanna. *J Geophys Res* 111:G02008.

Baldocchi, D., et al. (2001), FLUXNET: A New Tool to Study the Temporal and Spatial Variability of Ecosystem scale Carbon Dioxide, Water Vapor, and Energy Flux Densities, *Bulletin of the American Meteorological Society*, 82(11), 2415–2434.

Berg AA (1997).Urban impacts on a prairie groundwater system: estimation of anthropogenic contributions of water and potential effects on water table development. Unpublished M.Sc. Thesis, University of Lethbridge, Lethbridge, AB, 208 pp

Betz, R., R. Lootens, and M. Becker. 1996. Two decades of prairie restoration at Fermilab Batavia, Illinois. Pages 20–30 in C. Warwick, editor. *Proceedings of the Fifteenth North American Prairie Conference*. The Natural Areas Association, Bend, Oregon.

Betz, R.F. 1986. One decade of research in prairie restoration at the Fermi National Accelerator Laboratory (Fermilab), Batavia, Illinois. p. 179–185. In G.K. Clambey, and R.H. Pemble (ed.) *The prairie: Past, present and future*. Proceedings of the Ninth North American Prairie Conference, Moorhead State University, Moorhead, MN.

Bonan G.B. 1996. A Land Surface Model (LSM Version 1.0) for Ecological, Hydrological and Atmospheric Studies: Technical Description and User 's Guide. NCAR Technical Note T.N.-417+STR. National Center for Atmospheric Research, Boulder, CO.

Bonan, G., 2002: *Ecological Climatology: Concepts and Applications*. Cambridge University Press, 678 pp.

Borchert R, Rivera G (2001) Photoperiodic control of seasonal development and dormancy in tropical stem-succulent trees. *Tree Physiology*, 21, 213–221.

Canadell, J. G., and Coauthors, 2003: Science framework and implementation. *Earth System*

Science Partnership (IGBP, IHDP, WCRP, DIVERSITAS) Rep. 1 and Global Carbon Project Rep. 1, 69 pp.

Canadell, J., R.B. Jackson, J.R. Ehleringer, H.A. Mooney, O.E. Sala, E.D. Schulze, 1996, Maximum rooting depth of vegetation types at the global scale. *Oecologia*, 108(4), 583-595.

Cannell, M.G.R. and Smith, R.I. 1983. Thermal time, chill days, and prediction of budburst in *Picea sitchensis*. *J. Appl. Ecol.* 20: 951-963.

Carlson PJ (2000). Seasonal and inter-annual variation in carbon dioxide exchange and carbon balance in a mixed grassland. Unpublished M.Sc. Thesis, University of Lethbridge, Lethbridge, AB.

Childe SL (1989) Phenology of nine common woody species in semi-arid, deciduous Kalahari Sand vegetation. *Vegetatio*, 79, 151-163.

Chuine, I. and Cour, P. 1999. Climatic determinants of budburst seasonality in four temperate-zone tree species. *New Phytol.* 143: 339-349.

Clapp, R. B., and G. M. Hornberger (1978), Empirical Equations for some Soil Hydraulic Properties, *Water Resources Research*, 14(4), 601-604.

Collatz, G.J., J.T. Ball, C. Grivet, J.A. Berry (1991), Physiological and Environmental Regulation of Stomatal Conductance, Photosynthesis and Transpiration: A Model that Includes a Laminar Boundary Layer. *Agr. Forest Meteorol.*, 54, 107-136.

Collatz, G.J., M. Ribas-Carbo, J.A. Berry (1992), Coupled Photosynthesis-Stomatal Conductance Model for Leaves of C4 Plants. *Aust. J. Plant Physiol.*, 19(5), 519-538.

Cosby, B. J., G. M. Hornberger, R. B. Clapp, and T. R. Ginn (1984), A Statistical Exploration of the Relationships of Soil Moisture Characteristics to the Physical Properties of Soils, *Water Resour. Res.*, 20(6), 682–690, doi: 10.1029/WR020i006p00682.

Dai, Y., X. Zeng, R.E. Dickinson, I. Baker, G. Bonan, M. Bosilovich, S. Denning, P. Dirmeyer, P. Houser, G. Niu, K. Oleson, A. Schlosser and Z.-L. Yang (2003), The common land model (CLM). *B. Am. Meteorol. Soc.*, 84, 1013-1023.

de Bie S, Ketner P, Paasse M et al. (1998) Woody plant phenology in the West Africa savanna. *Journal of Biogeography*, 25, 883–900.

De Deyn, G. B., Cornelissen, J. H. C., and Bardgett, R. D. (2008). Plant functional traits and soil carbon sequestration in contrasting biomes. *Ecology Letters* 11, 516-531.

Dickinson, R. E., Y. Tian, Q. Liu, and L. Zhou (2008), Dynamics of leaf area for climate and weather models, *J. Geophys. Res.*, 113, D16115, doi:10.1029/2007JD008934.

Do, F.C., Goudiaby, V.A., Gimenez, O., Diagne, A.L., Mayecor, D., Rocheteau, A. and Akpo, L.E. 2005. Environmental influence on canopy phenology in the dry tropics. *For. Ecol. Manage.* 215: 319-328.

Douville, H., 2003: Assessing the influence of soil moisture on seasonal climate variability with AGCMs. *J. Hydrometeor.*, 4, 1044–1066.

Dye, P.J. and Walker, B.H. 1987. Patterns of shoot growth in a semi-arid grassland in Zimbabwe. *J. Appl. Ecol.* 24: 633-644.

Environment Canada (2010a). Canadian Climate Normals and Averages: 1971–2000. Available at: http://climate.weatheroffice.ec.gc.ca/climate-normals/index_e.html (accessed 24 August 2010).

Flanagan LB , WeverLA, CarlsonPJ (2002) Seasonal and interannual variation in carbon dioxide exchange and carbon balance in a northern temperate grassland. *Global Change Biology*, **8**, 599–615.

Flanagan LB, Johnson BG (2005) Interacting effects of temperature, soil moisture and plant biomass production on ecosystem respiration in a northern temperate grassland. *Agricultural and Forest Meteorology*, **130**, 237–253

Flangan L. B. and Adkinson, A. C. (2011), Interacting controls on productivity in a northern Great Plains grassland and implications for response to ENSO events. *Global Change Biology*, **17**: 3293–3311. doi: 10.1111/j.1365-2486.2011.02461.x

Friedlingstein, P.F., P. Cox, R. Betts, L. Bopp, W. von Bloh, V. Brovkin, P. Cadule, S. Doney, M. Eby, I. Fung, G. Bala, J. John, C. Jones, F. Joos, T. Kato, M. Kawamiya, W. Knoff, K. Lindsay, H.D. Matthews, T. Raddatz, P. Rayner, C. Reick, E. Roeckner, K.-G. Schnitzler, R. Schnur, K. Strassmann, A.J. Weaver, C. Yoshikawa, N. Zeng, (2006), Climate-carbon cycle feedback analysis: Results from the C4MIP model intercomparison, *J. Clim.*, **19**, 3337-3353.

Gash JHC (1986) A note on estimating the effect of a limited fetch on micrometeorological evaporation measurements. *Bound-Layer Meteor* **35**:409-13

Gibson, J. David, 2009: Grasses and grassland ecology. Oxford University Press, 305pp

Gomez-Casanovas N, Matamala R, Cook DR, Gonzalez-Meler MA (2012) Net ecosystem exchange modifies the relationship between the autotrophic and heterotrophic components of soil respiration with abiotic factors in prairie grasslands. *Global Change Biology*, **18**, 2532–2545.

Görzen, K., A. H. Lynch, A. G. Marshall, and J. Beringer, 2006: Impact of abrupt land cover changes by savanna fire on northern Australian climate. *J. Geophys. Res.*, **111**, D19106, doi:10.1029/2005JD006860.

Grace, J., San José, J., Meir, P., Miranda, H. S., and Montes, R. A. (2006). Productivity and carbon fluxes of tropical savannas. *Journal of Bio- geography* 33, 387-400.

Hansen, M. C., R. S. DeFries, J. R. G. Townshend, and R. Sohlberg, 2000: Global land cover classification at 1km spatial resolution using a classification tree approach. *Int. J. Remote Sens.*, 21, 1331–1364.

Harper B A. (2011) PhD Dissertation: Drought tolerance and implications for vegetation-climate interactions in the Amazon forest. Colorado State University, Fort Collins, Colorado

Hsieh CI, Katul G, Chi T (2000) An approximate analytical model for footprint estimation of scalar fluxes in thermally stratified atmospheric flows. *Adv Water Resour* 23(7):765–772

Huxman TE et al (2004) Precipitation pulses and carbon fluxes in semiarid and arid ecosystems. *Oecologia* 141:254–268

IPCC (2007), Climate Change 2007. *The Physical Science Basis. Contribution of Working Group I to the Fourth Assessment Report of the Intergovernmental Panel on Climate Change* [Solomon, S., D. Qin, M. Manning, Z. Chen, M. Marquis, K.B. Averyt, M. Tignor and H.L. Miller (eds.)]. Cambridge University Press, Cambridge, United Kingdom and New York, USA, 996 pp.

Jackson, R.B., J. Canadell, J.R. Ehleringer, H.A. Mooney, O.E. Sala, E.D. Schulze (1996), A global Analysis of root distributions for terrestrial biomes. *Oecologia*, 108, 389-411.

Jarvis P, Linder S. 2000. Constraints to growth of boreal forests. *Nature* 405: 904–905.

Jenerette GD, Scott RL, Huxman TE (2008) Whole ecosystem metabolic pulses following precipitation events. *Funct Ecol* 22:924–930

Jolly, W. M., R. Nemani, and S. W. Running (2005), A generalized, bio-climatic index to predict foliar phenology in response to climate, *Global Change Biol.*, 11, 619–632.

Jolly, W.M. and Running, S.W. 2004. Effects of precipitation and soil water potential on drought deciduous phenology in the Kalahari. *Global Change Biol.* 10: 303-308.

Keeling, C.D., T.P. Whorf, M. Whalen and J.van der Plicht, 1995. Interannual extremes in the rate of rise of atmospheric carbon dioxide since 1980. *Nature*, 375, 666-670.

Lattanzi Fa (2010) C3/C4 grasslands and climate change. *Grassland Science in Europe* 15, 3-13.

Law, B.E., Bakwin, P.S., Baldocchi, D.D., Boden, T., Davis, K.J., Hollinger, D., Munger, W.J., Nobre, A., Running, S.W., Wofsy, S.C., Verma, S., 2003. The AmeriFlux network paradigm for measuring and understanding the role of the terrestrial biosphere in global climate change. *Bioscience*, (submitted for publication).

Los, S. O., et al. (2000), A global 9_yr biophysical land surface dataset from NOAA AVHRR data, *J. Hydrometeorol.*, 1, 183–199.

Lynch, A. H., D. Abramson, K. Görgen, J. Beringer, and P. Uotila, 2007: Influence of savanna fire on Australian monsoon season precipitation and circulation as simulated using a distributed computing environment. *Geophys. Res. Lett.*, 34, L20801, doi:10.1029/2007GL030879.

Matamala, R.; Jastrow, J. D.; Miller, R. M.; Garten, C. T. 2008. Temporal changes in C and N stocks of restored prairie: Implications for C sequestration strategies. *Ecological Applications* 18: 1470-1488.

McWilliam, A-L.C., Cabral, O.M.R., Gomes, B.M., Esteves, J.L., Roberts, J.M., 1996. Forest and pasture leaf-gas exchange in south-west Amaz"nia. In 'Amazon Deforestation and Climate' (Eds. J.H.C.Gash, C.A.Nobre, J.M.Roberts and R.L.Victoria). John Wiley, Chichester, UK. pp 265-286.

Milton, S. J. 1987. Phenology of seven *Acacia* species in South Africa. *S. Afr. J. Wildlife Res.* 17: 1-6.

Mistry, J., 2000: World Savannas: Ecology and Human Use. Longman Group, 352 pp

Monsi, M., and T. Saeki (2005), On the factor light in plant communities and its importance for matter production, *Ann. Bot.*, 95, 549–567.

Myneni RB, Keeling CD, Tucker CJ et al. (1997) Increased plant growth in the northern high latitudes from 1981–1991. *Nature*, 386, 698–702.

Nizinski, J. J. and Saugier, B. 1988. A model of leaf budding and development for a mature *Quercus* forest. *J. Appl. Ecol.* 25: 643-652.

Njoku E (1958) The photoperiodic response of some Nigerian plants. *Journal of the West African Science Association*, 4, 99–111.

Ostlie WR, Schneider RE, Aldrich JM, Faust TM, McKim RLB, Chaplin SJ (1997) The Status of Biodiversity in the Great Plains. The Nature Conservancy, Arlington, VA.

Owen-Smith, N. and Cooper, S. M. (1989). Nutritional ecology of a browsing ruminant, the kudu (*Tragelaphus strepsiceros*), through the seasonal cycle. *Journal of Zoology* 219, 29–43.

Pitman, A. J., 2003: The evolution of, and revolution in, land surface schemes designed for climate models. *Int. J. Climatol.*, 23, 479–510.

Porporato A, Laio F, Ridolfi L, Rodriguez-Iturbe I (2001) Plants in water-controlled ecosystems: active role in hydrologic processes and response to water stress. III. Vegetation water stress. *Adv Water Resour* 24:725–744

Prins, H.H.T. 1988. Plant phenology patterns in Lake Manyara National Park, Tanzania. *J. Biogeogr.* 15: 465-480.

Randall, D. A., and Coauthors, 2007: Climate models and their evaluation. Climate Change 2007: The Physical Science Basis, S. Solomon et al., Eds., Cambridge University Press, 589–662.

Randall, D.A., D.A. Dazlich, C. Zhang, A.S. Denning, P.J. Sellers, C.J. Tucker, L. Bounoua, J.A. Berry, G.J. Collatz, C.B. Field, S.O. Los, C.O. Justice, I. Fung (1996), A Revised Land Surface Parameterization (SiB2) for GCMs. Part III: The Greening of the Colorado State University General Circulation Model. *J. Climate*, 9(4), 738-763.

Reed, B.C., Brown, J.F., VanderZee, D., Loveland, T.R., Mer- chant, J.W. and Ohlen, D.O. 1994. Measuring phenological variability from satellite imagery. *J. Veg. Sci.* 5: 703-714.

Reich, P.B. and Borchert, R. 1984. Water stress and tree phenology in a tropical dry forest in the lowlands of Costa Rica. *J. Ecol.* 72: 61-74.

Richardson AD, Anderson RS, Arain MA et al., 2012: Terrestrial biosphere models need better representation of vegetation phenology: results from the North American Carbon Program Site Synthesis. *Global Change Biology*, 18, 566–584

Roberts, J.M., Cabral, O.M.R., da Costa, J.P., McWilliam, A-L.C. and Sa, T.D.A, 1996. An overview of the leaf area index and physiological measurements during ABRACOS. In 'Amazon Deforestation and Climate' (Eds. J.H.C.Gash, C.A.Nobre, J.M.Roberts and R.L.Victoria). John Wiley, Chichester, UK. pp 287-306.

Rodriguez-Iturbe I, Porporato A, Ridolfi L, Isham V, Cox DR (1999) Probabilistic modelling of water balance at a point: the role of climate, soil and vegetation. Proc R Soc Lond Ser A Math Phys Eng Sci 455:3789–3805

Savage C (2004) Prairie: a Natural History. Greystone Books, Douglas and McIntyre Publishing Group, Vancouver, BC.

Schimel D. S. (2006) Terrestrial ecosystems and the carbon cycle Global Change Biology 04/2006; 1(1):77 - 91. · 6.86 Impact Factor

Schmidt, A., C. Hanson, J. Kathilankal, and B.E. Law. 2011. Classification and assessment of turbulent fluxes above ecosystems in North-America with self-organizing feature map networks. *Agricultural and Forest Meteorology* 151(4): 508-520, doi:<http://dx.doi.org/10.1016/j.agrformet.2010.12.009>

Scholes, R. J., and S. Archer, 1997: Tree-grass interactions in savannas. Annu. Rev. Ecol. Syst., 28, 517–44.

Scholes, R.J. and Walker, B.H. 1993. *An African savanna: a synthesis of the Nylsvlei study*. Cambridge University Press, Cambridge, UK.

Schwartz MD, Reiter BE. 2000. Changes in North American spring. International Journal of Climatology 20: 929–932.

Scracek O (1993). Hydrogeology and hydrogeochemistry of buried preglacial valleys in the Lethbridge area, southern Alberta. Unpublished M.Sc. Thesis, University of Waterloo, Waterloo, ON.

Scurlock, J. M. O. and Hall, D. O. (1998). The global carbon sink: a grass- land perspective. Global Change Biology 4, 229-233.

Sea W.B., P. Choler, J. Beringer, R.A. Weinmann, L.B. Hutley, R. Leuning Documenting improvement in leaf area index estimates from MODIS using hemispherical photos for Australian savannas *Agricultural and Forest Meteorology*, 151 (2011), pp. 1453–1461

Seiwa, K. 1999. Changes in leaf phenology are dependent on tree height in *Acer mono*, a deciduous broad-leaved tree. *Ann. Bot.* 83: 355-361.

Sellers, P. J., Dickinson, R. E., Randall, D. A., Betts, A. K., Hall, F. G., Berry, J. A., Collatz, G. J., Denning, A. S., Mooney, H. A., Nobre, C. A., Sato, N., Field, C. B., and Henderson-Sellers, A. (1997). Modeling the exchanges of energy, water, and carbon between continents and the atmosphere. *Science*, 275(5299), 502 – 509.

Sellers, P. J., S. O. Los, C. J. Tucker, C. O. Justice, D. A. Dazlich, G. J. Collatz, and D. A. Randall, 1996b: A Revised Land Surface Parameterization (SiB2) for Atmospheric GCMS. Part II: The Generation of Global Fields of Terrestrial Biophysical Parameters from Satellite Data. *J. Climate*, 9, 706-737.

Sellers, P. J., Y. Mintz, Y. C. Sud, and A. Dalcher, 1986: A Simple Biosphere Model (SiB) for Use within General Circulation Models. *J. Atmos. Sci.*, 43, pp. 505-531, 1986.

Sellers, P.J. D.A. Randall, G.J. Collatz, J.A. Berry, C.B. Field, D.A. Dazlich, C. Zhang, G.D. Colello, L. Bounoua (1996a), A Revised Land Surface Parameterization (SiB2) for Atmospheric GCMs. Part I: Model Formulation. *J. Climate*, 9(4), 676-705.

Sellers, P.J., 1985: Canopy Reflectance, Photosynthesis and Respiration. *Int. J. Remote Sensing*, 6(8) 1335-1372

Sellers, P.J., 1987, Canopy reflectance, photosynthesis, and Transpiration. 2. The role of biophysics in the linearity of the interdependence. *Remote Sens. Environ.*, 21(2), 143-183.

Sellers, P.J., J.A. Berry, G.J. Collatz, C.B. Field, F.G. Hall (1992), Canopy Reflectance, Photosynthesis, and Transpiration. III. A Reanalysis Using Improved Leaf Models and a New Canopy Integration Scheme. *Remote Sens. Environ.*, 42, 1878-216.

Shackleton, C.M. 1999. Rainfall and topo-edaphic influences on woody community phenology in South African savannas. *Global Ecol. Biogeogr.* 8: 125-136.

Silver, W.L., Neff, J., McGroddy, M., Veldkamp, E., Keller, M., Cosme, R., 2000, Effects of Soil Temperature on Belowground Carbon and Nutrient Storage in a Lowland Amazonian Forest Ecosystem, *Ecosystems*, 3, 193-209.

Singh, K.P. and Kushwaha, C.P. 2005. Emerging paradigms of tree phenology in dry tropics. *Curr. Sci.* 89: 964-975.

Solomon, S., G.-K. Plattner, R. Knutti and P. Friedlingstein, 2009, Irreversible climate change due to carbon dioxide emissions. *P. Nat. Acad. Sci. USA*, 106(6), doi:10.1073/pnas.0812721106.

Stöckli, R., D. M. Lawrence, G.-Y. Niu, K. W. Oleson, P. E. Thornton, Z.-L. Yang, G. B. Bonan, A. S. Denning, and S. W. Running (2008), Use of FLUXNET in the Community Land Model development, *J. Geophys. Res.*, 113, G01025, doi:10.1029/2007JG000562.

Stöckli, R., T. Rutishauser, D. Dragoni, J. O'Keefe, P. E. Thornton, M. Jolly, L. Lu, and A. S. Denning (2008b), Remote sensing data assimilation for a prognostic phenology model, *J. Geophys. Res.*, 113, G04021, doi:10.1029/2008JG000781.

Stöckli, R., T. Rutishauser, I. Baker, M. A. Liniger, and A. S. Denning (2011), A global reanalysis of vegetation phenology, *J. Geophys. Res.*, 116, G03020, doi:10.1029/2010JG001545.

Suyker, A.E., and S.B. Verma. 2001. Year-round observations of the net ecosystem exchange of carbon dioxide in a native tallgrass prairie. *Global Change Biology* 7(3): 279-289, doi:<http://dx.doi.org/10.1046/j.1365-2486.2001.00407.x>

Tucker C.J., Pinzon J.E., Brown M.E., Slayback D.A., Pak E.W., Mahoney R., Vermote E.F., and El Saleous N.. "An Extended AVHRR 8-km NDVI Data Set Compatible with MODIS and SPOT Vegetation NDVI Data", *International Journal of Remote Sensing*, 26 (20): 4485-4498, 2005.

Wever LA , FlanaganLB, CarlsonPJ (2002) Seasonal and interannual variation in evapotranspiration, energy balance and surface conductance in a northern temperate grassland. *Agricultural and Forest Meteorology*, **112**, 31–49.

White MA, Thornton PE, Running SW (1997) A continental phenology model for monitoring vegetation responses to interannual climatic variability. *Global Biogeochemical Cycles*, 11, 217–234.

Williams, C. A. et al. 2009, Complexity in water and carbon dioxide fluxes following rain pulses in an African savanna, *Oecologia*, Volume 161, Issue 3, pp 469-480.

Williams, C. A., and J. D. Albertson (2004), Soil moisture controls on canopy-scale water and carbon fluxes in an African savanna, *Water Resour. Res.*, 40, W09302, doi:10.1029/2004WR003208.

Wilson, T. and Meyers, T.: Determining vegetation indices from solar and photosynthetically active radiation fluxes, *Agr. For. Meteorol.*, 144(3–4), 160–179, 2007.

Woodward, F. I., Lomas, M. R., and Kelly, C. K. (2004). Global climate and the distribution of plant biomes. *Philosophical Transactions of the Royal Society B: Biological Sciences* 359, 1465-1476.

Xu Liukang, Baldocchi Dennis D. 2004, Seasonal variation in carbon dioxide exchange over a Mediterranean annual grassland in California, Agricultural and Forest Meteorology, Volume 123, Issues 1–2, Pages 79-96.

Xu LK, Baldocchi DD, Tang JW (2004) How soil moisture, rain pulses, and growth alter the response of ecosystem respiration to temperature. Global Biogeochem Cycles 18(4):GB4002

Zanchi, F.B.; Waterloo, M.J.; Aguiar, L.J.G.; Randon, C.V.; Kruijt, B.; Cardoso, F.L.; Manzi, A. O. Estimativa do Índice de Área Foliar (IAF) e Biomassa em pastagem no estado de Rondônia, Brasil. Acta Amazonica, v. 39, n.2, p.335-348, 2009.

Zhang L. et al. 2007, Evaluation and comparison of gross primary production estimates for the Northern Great Plains grasslands, Remote Sensing of Environment, Volume 106, Issue 2, Pages 173-189, ISSN 0034-4257, 10.1016/j.rse.2006.08.012.

Appendix A

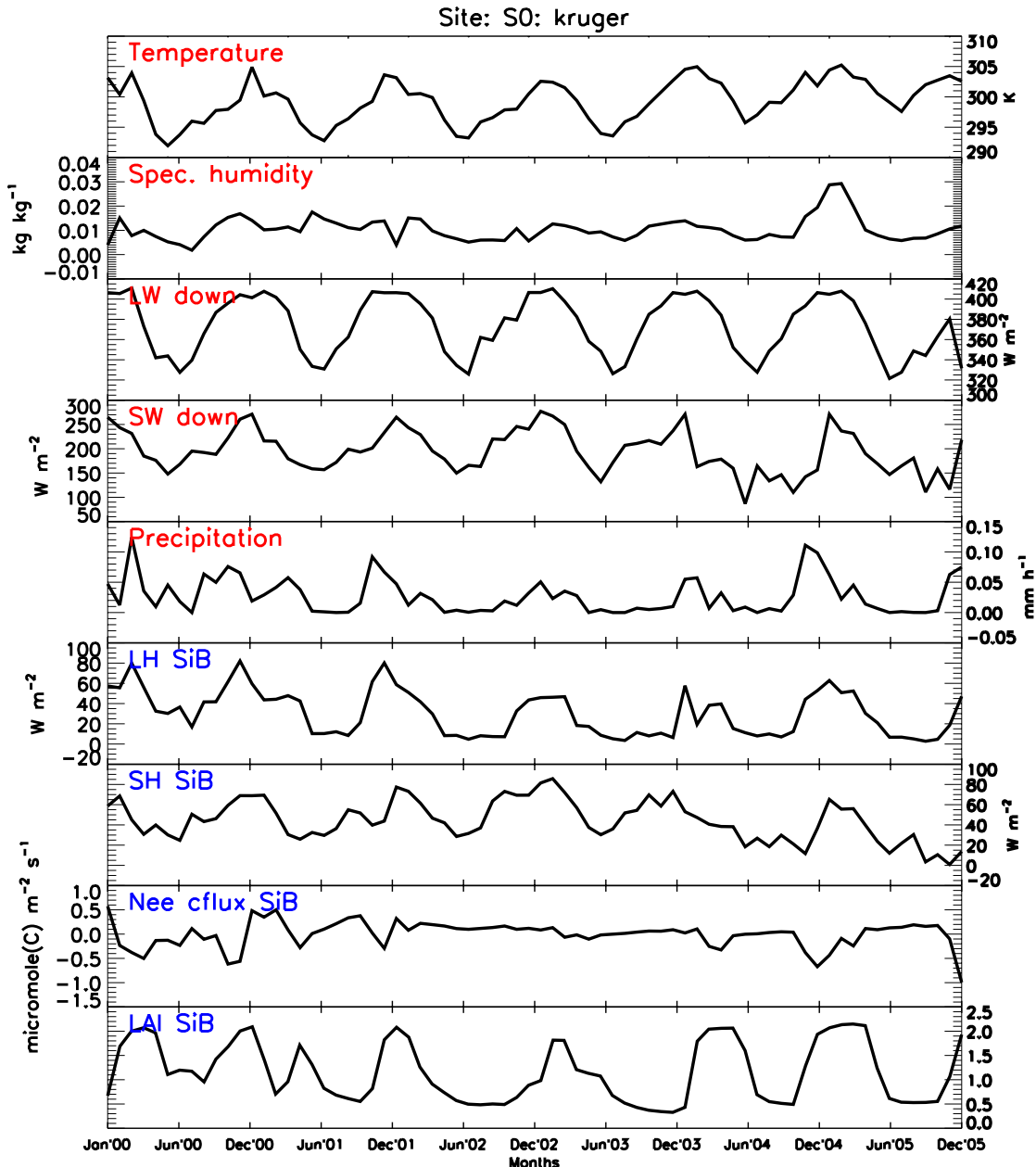


Figure 23 Monthly means of observed (red) and modeled (blue) variables at site S0 – Skukuza, Kruger Park, South Africa. LW – Long Wave radiation; SW – Short Wave radiation; SH Sensible Heat; LH – Latent Heat; Nee cflux SiB – carbon flux diagnosed by SiB; LAI – Leaf Area Index

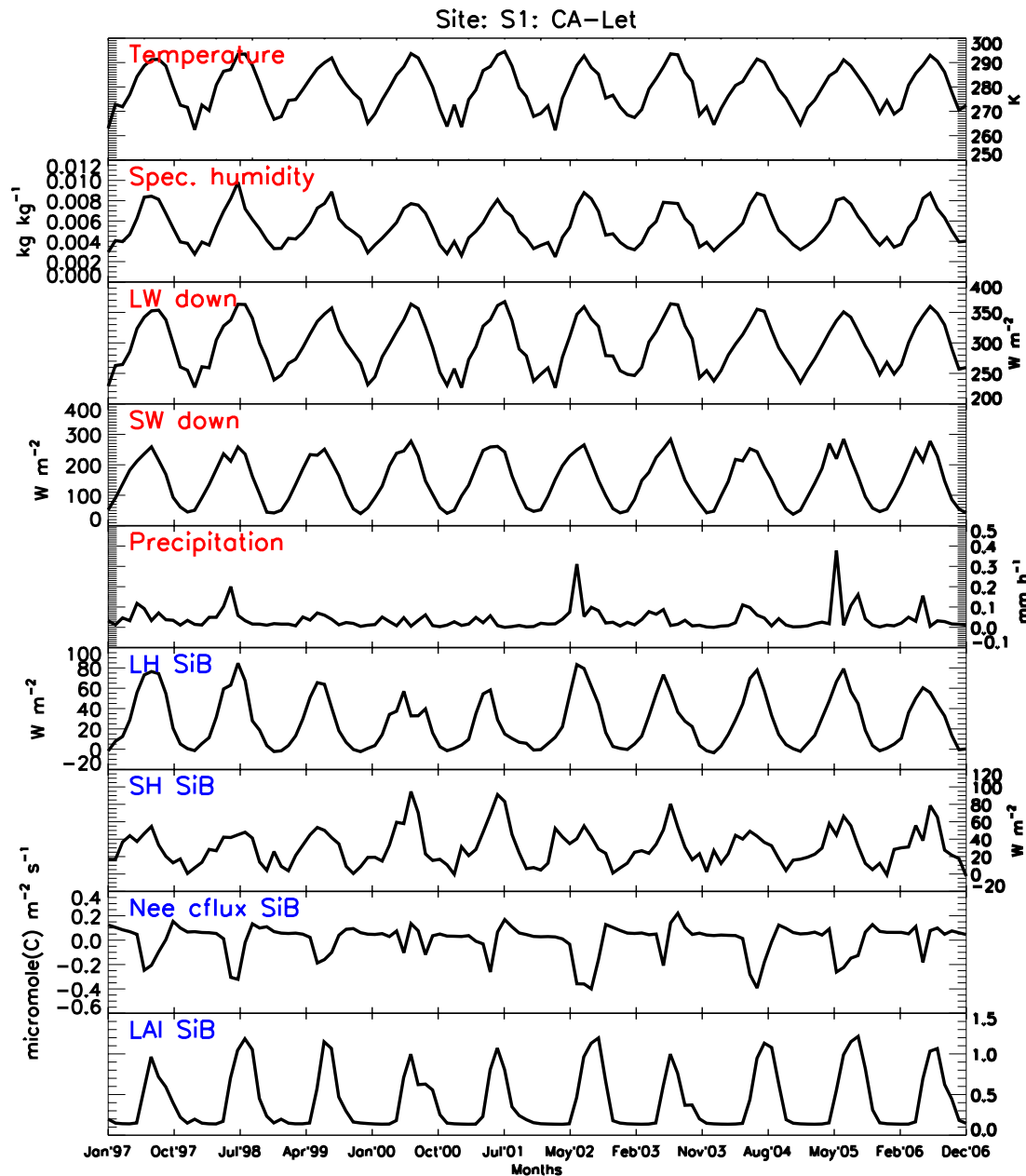


Figure 24 Monthly means of observed (red) and modeled (blue) variables at site S1 – Lethbridge, Canada. LW – Long Wave radiation; SW – Short Wave radiation; SH Sensible Heat; LH – Latent Heat; Nee cflux SiB – carbon flux diagnosed by SiB; LAI – Leaf Area Index

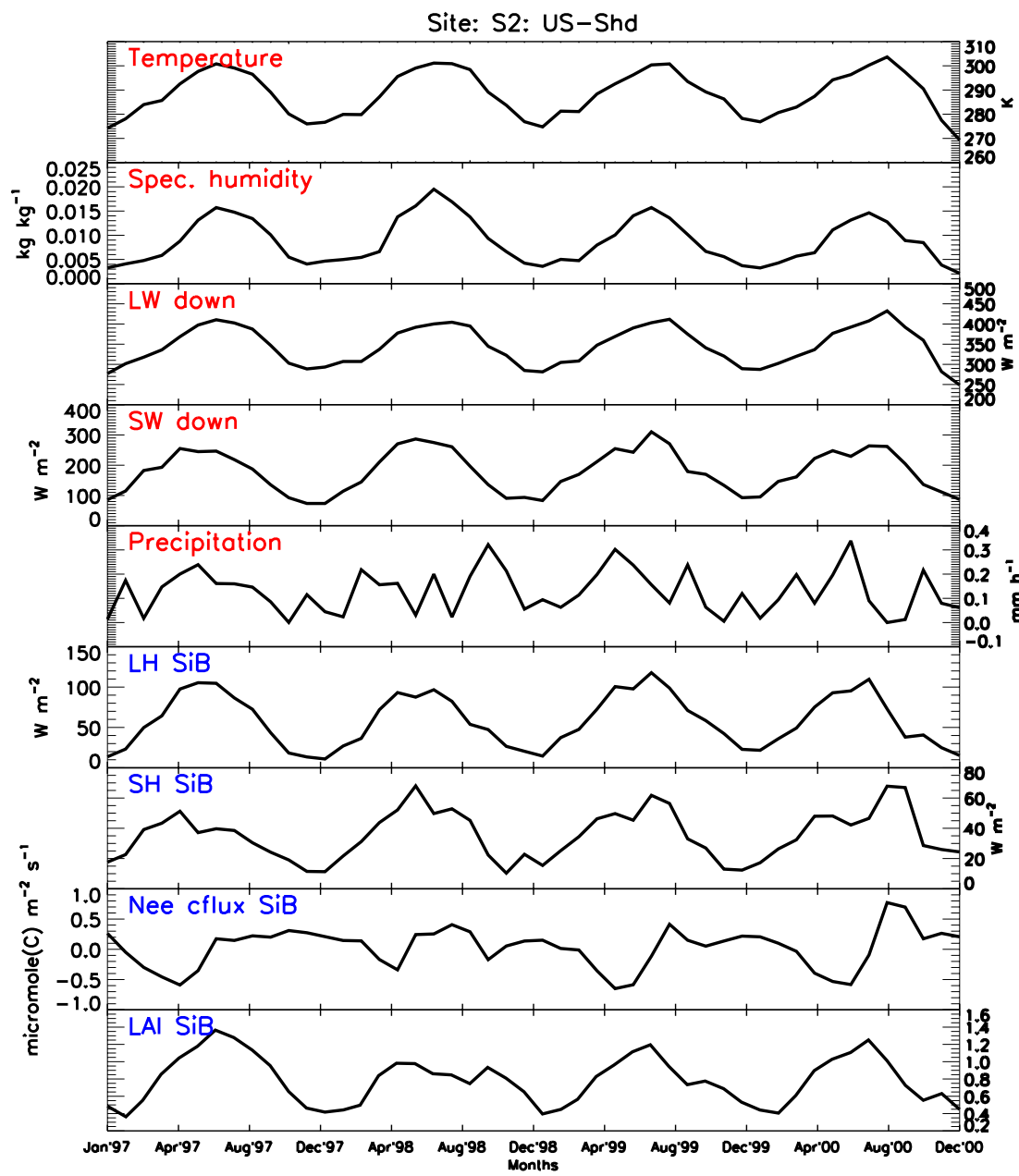


Figure 25 Monthly means of observed (red) and modeled (blue) variables at site S2 – Shidler Tallgrass Prairie, Oklahoma, US. LW – Long Wave radiation; SW – Short Wave radiation; SH Sensible Heat; LH – Latent Heat; Nee cflux SiB – carbon flux diagnosed by SiB; LAI – Leaf Area Index.

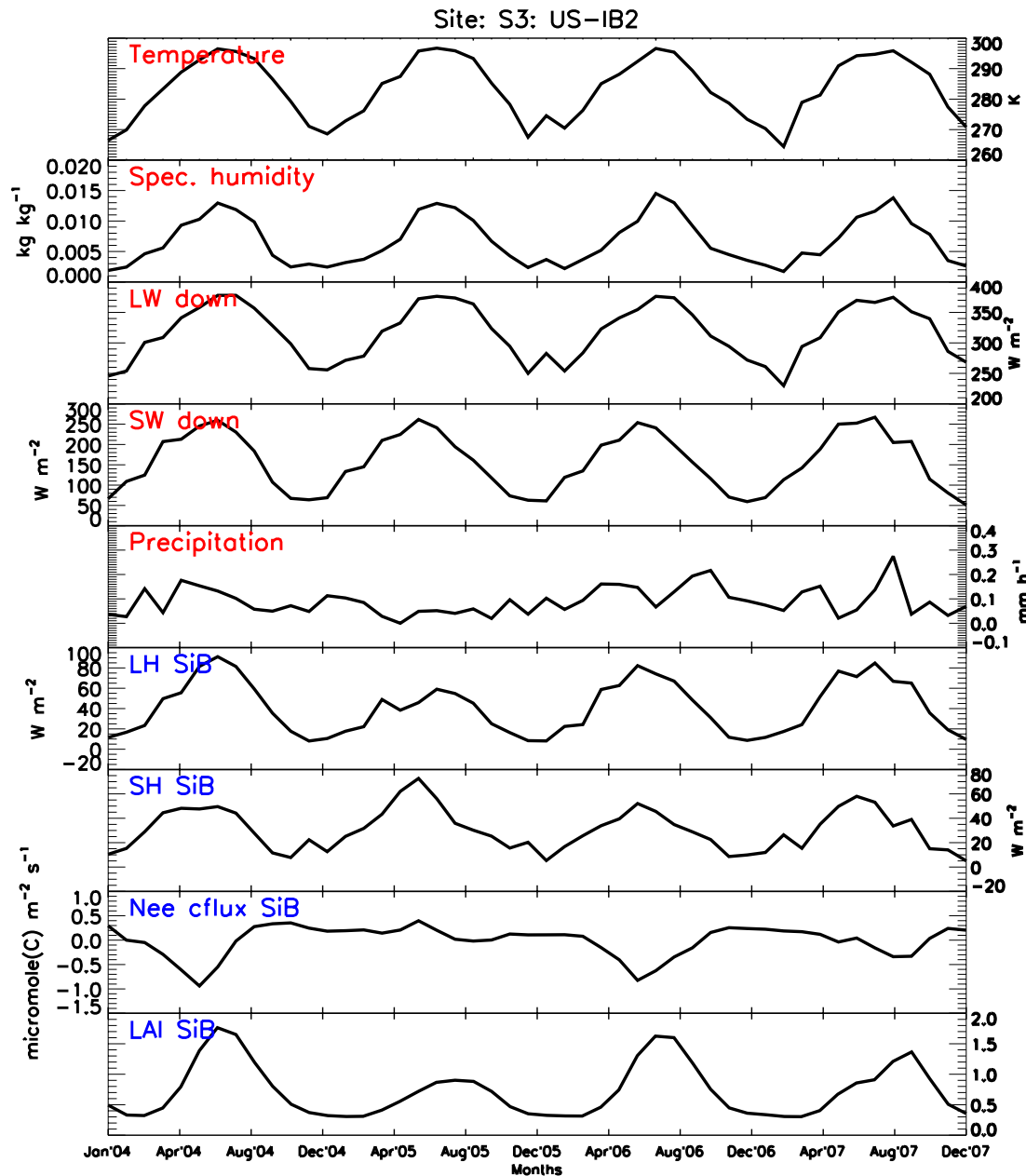


Figure 26 Monthly means of observed (red) and modeled (blue) variables at site S3 – Fermi Prairie, Illinois, US. LW – Long Wave radiation; SW – Short Wave radiation; SH Sensible Heat; LH – Latent Heat; Nee cflux SiB – carbon flux diagnosed by SiB; LAI – Leaf Area Index.

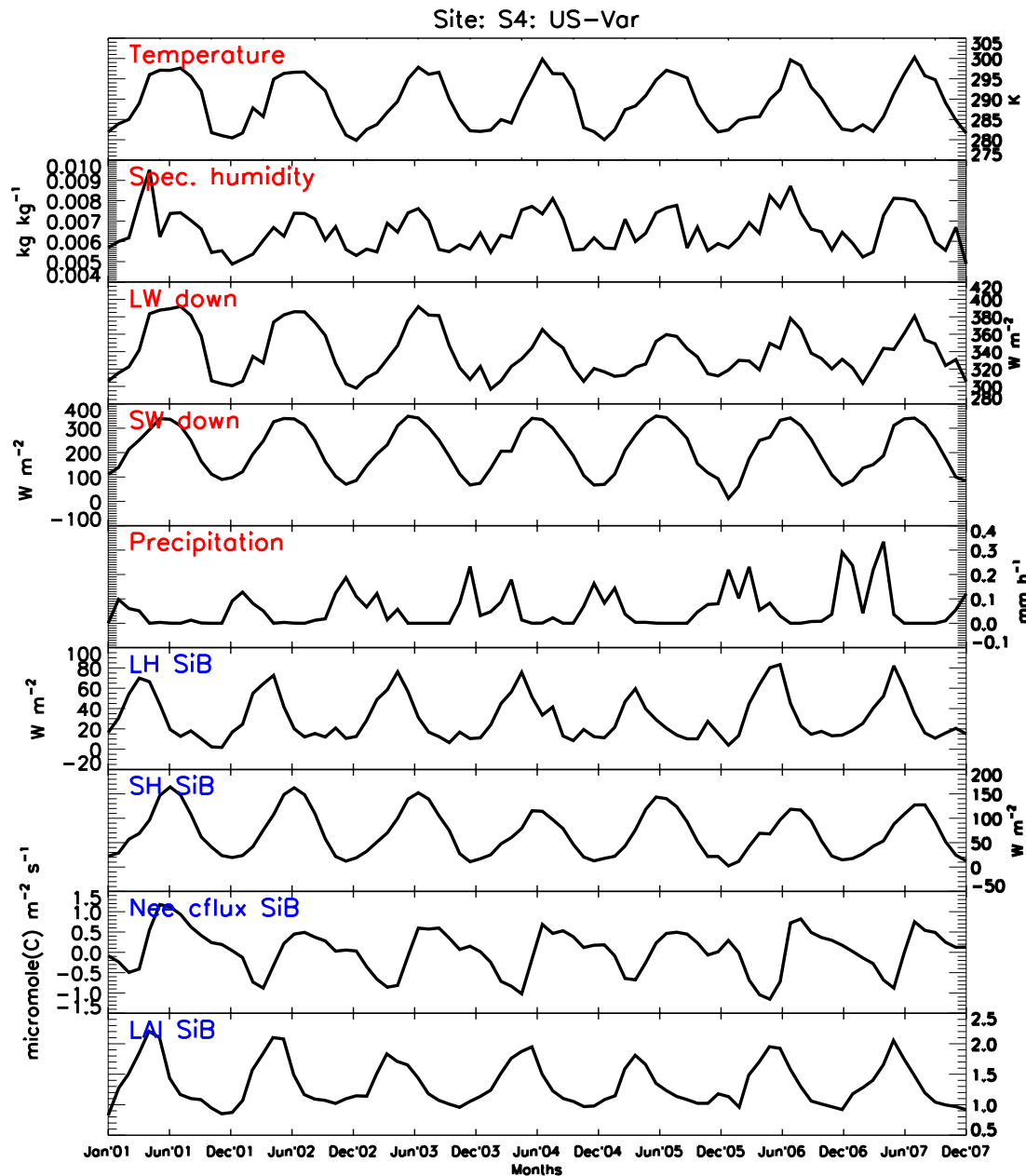


Figure 27 Monthly means of observed (red) and modeled (blue) variables at site S4 – Vaira Ranch, California, US. LW – Long Wave radiation; SW – Short Wave radiation; SH Sensible Heat; LH – Latent Heat; Nee cflux SiB – carbon flux diagnosed by SiB; LAI – Leaf Area Index.

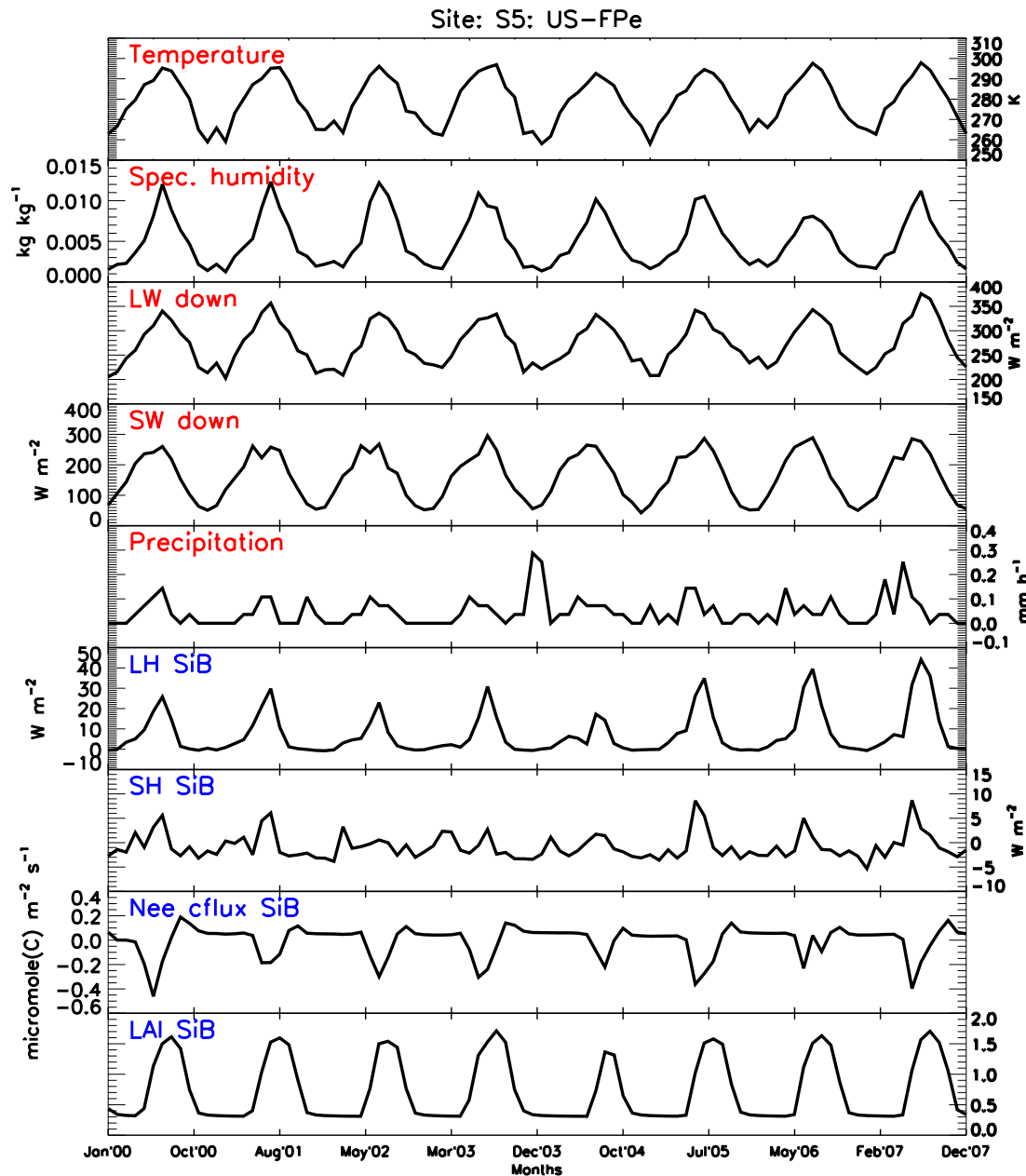


Figure 28 Monthly means of observed (red) and modeled (blue) variables at site S5 – Fort Peck, Montana, US. LW – Long Wave radiation; SW – Short Wave radiation; SH Sensible Heat; LH – Latent Heat; Nee cflux SiB – carbon flux diagnosed by SiB; LAI – Leaf Area Index.

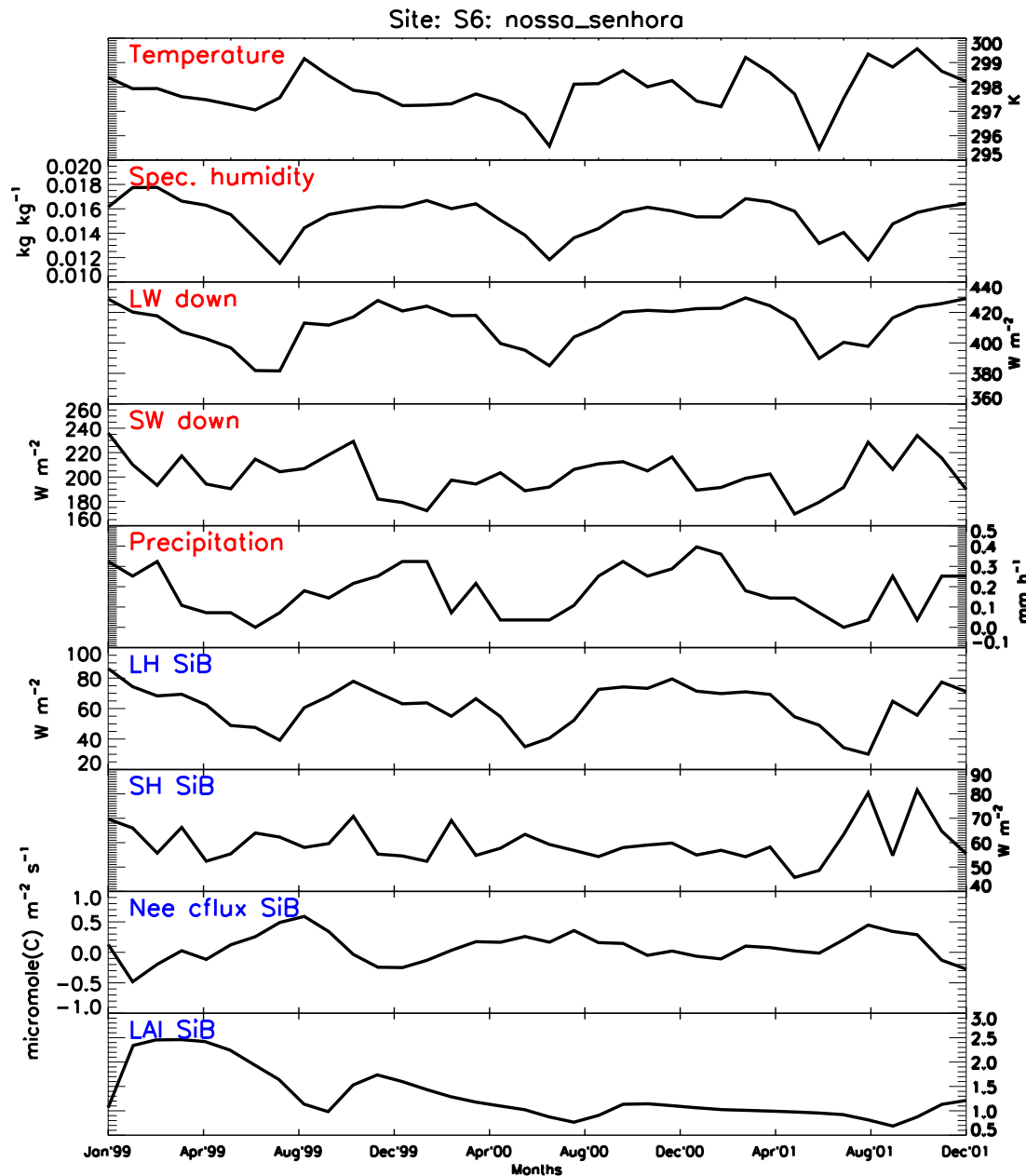


Figure 29 Monthly means of observed (red) and modeled (blue) variables at site S6 – Fazenda Nossa Senhora, Brazil. LW – Long Wave radiation; SW – Short Wave radiation; SH Sensible Heat; LH – Latent Heat; Nee cflux SiB – carbon flux diagnosed by SiB; LAI – Leaf Area Index.

Appendix B

A list of plant functional types (PFTs) defined in the phenology subroutine of SiB3 is given in Table B-0-1 followed by tables of vegetation distributions at seven sites presented in this study. Details on definitions of the PFTs can be found at Bonan (2002) while description and methodology of defining spatial distribution of PFTs is described and referenced in Stöckli (2008, 2011). Differences between most common PFT's in grasslands, such as C3 and C4 grass are given by Lattanzi (2010).

Table 4 A List of 35 phenology types allowed in SiB's phenology model

Bare Soil (-)	Crops (Groundnuts)
Evergreen Needleleaf Trees (Temperate)	Crops (Maize)
Evergreen Needleleaf Trees (Boreal)	Crops (Millet)
Deciduous Needleleaf Trees (Boreal)	Crops (Oilpalm)
Evergreen Broadleaf Trees (Tropical)	Crops (Other)
Evergreen Broadleaf Trees (Temperate)	Crops (Potato)
Deciduous Broadleaf Trees (Tropical)	Crops (Pulses)
Deciduous Broadleaf Trees (Temperate)	Crops (Rape)
Deciduous Broadleaf Trees (Boreal)	Crops (Rice)
Evergreen Broadleaf Shrubs (All)	Crops (Rye)
Deciduous Broadleaf Shrubs (Temperate)	Crops (Sorghum)
Deciduous Broadleaf Shrubs (Boreal)	Crops (Soy)
C3 Grass (Arctic)	Crops (Sugarbeets)
C3 Grass (Non-Arctic)	Crops (Sugarcane)
C4 Grass (All)	Crops (Sunflower)
Crops (Barley)	Crops (Wheat)
Crops (Cassava)	Water (All)
Crops (Cotton)	

Table 5 Distribution of phenological functional types present at site S0 – Skukuza, Kruger Park, South Africa

Phenological functional types	Percent of coverage (%)
Grass C4	58.7
Grass C3 Non-Arctic	9.2
Deciduous Broadleaf Trees (tropical)	12.3
Deciduous Broadleaf Shrubs (temperate)	12.7
Bare Ground	7.1

Table 6 Distribution of phenological functional types present at S1 – Lethbridge, Canada

Phenological functional types	Percent of coverage (%)
Bare Soil	23.9
Deciduous Broadleaf Trees (Temperate)	1.0
C3 Grass (Non-Arctic)	42.1
Crops (Barley)	8.9
Crops (Other)	2.8
Crops (Pulses)	1.0
Crops (Rape)	6.4
Crops (Wheat)	13.9

Table 7 Distribution of phenological functional types present at site S2 - Shidler Tallgrass Prairie, Oklahoma, US

Phenological functional types	Percent of coverage (%)
Bare Soil	10.9
Evergreen Needleleaf Trees (Temperate)	1.6
Deciduous Broadleaf Trees (Temperate)	5.3
Deciduous Broadleaf Shrubs (Temperate)	1.2
C3 Grass (Non-Arctic)	13.4
C4 Grass (All)	34.4
Crops (Maize)	0.2
Crops (Sorghum)	0.6
Crops (Soy)	0.8
Crops (Wheat)	4.2
Water (All)	0.3

Table 8 Distribution of phenological functional types present at site S3- Fermi Prairie, Illinois, US

Phenological functional types	Percent of coverage (%)
Bare Soil	4.2
Evergreen Needleleaf Trees (Temperate)	1.6
Deciduous Broadleaf Trees (Temperate)	7.8
C3 Grass (Non-Arctic)	10.7
C4 Grass (All)	8.1
Crops (Maize)	34.0
Crops (Other)	1.4
Crops (Sorghum)	0.6
Crops (Soy)	27.6
Crops (Wheat)	4.1

Table 9 Distribution of phenological functional types present at site S4 – Vaira Ranch, California, US

Phenological functional types	Percent of coverage (%)
Bare Soil	3.2
Evergreen Needleleaf Trees (Temperate)	4.4
Deciduous Broadleaf Trees (Temperate)	8.2
Evergreen Broadleaf Shrubs (All)	24.7
C3 Grass (Non-Arctic)	58.3
Crops (Other)	0.1

Table 10 Distribution of phenological functional types present at site S5 – Fort Peck, Montana, US

Phenological functional types	Percent of coverage (%)
Bare Soil	31.1
C3 Grass (Non-Arctic)	28.4
Crops (Barley)	8.1
Crops (Maize)	0.1
Crops (Other)	1.0
Crops (Pulses)	0.1
Crops (Rape)	0.8
Crops (Wheat)	30.3

Table 11 Distribution of phenological functional types present at site S6 – Fazenda Nossa Senhora, Brazil

Phenological functional types	Percent of coverage (%)
Evergreen Broadleaf Trees (Tropical)	19.0
Deciduous Broadleaf Trees (Tropical)	3.8
Deciduous Broadleaf Shrubs (Temperate)	9.6
C3 Grass (Non-Arctic)	1.8
C4 Grass (All)	62.2
Crops (Maize)	1.0
Crops (Other)	1.1
Crops (Pulses)	0.8
Crops (Rice)	0.8